Regulation and Effect of Endothelial Acetylcholine on Oligodendrocyte Progenitor Cells

by

Roopa Ravichandar

July 12th 2019

A thesis submitted to the Faculty of the Graduate School of the University at Buffalo, The State University of New York, in partial fulfillment of the requirements for the degree of

Master of Science

Neuroscience Program

Acknowledgments

First and foremost, I would like to thank my mentor and advisor, Dr. Fraser Sim, for his constant guidance and endless support while pursuing my thesis. He has always been a wonderful source of encouragement and has demonstrated his kind efforts to bring out the best in me. I am very thankful to him for giving me the opportunity to work in his lab. I find it a true honor to be part of his lab and I am very excited for the next few years working as a PhD student under him.

I would like to thank my committee members Dr. Jennifer K. Lang and Dr. John Kolega for their invaluable suggestions in bringing this project to a good shape.

I would like to sincerely thank all the members of the Sim Lab: Darpan, Jackie, JP, Rich, James, Divyangi, Heba, Arsalan, Ahmed, Khushbu, BK, Beverly, Ein, Joanna who have all been extremely helpful in the course of my thesis work by giving me all the emotional support I needed. Thank you all for making this lab a fun place to work and learn. I am deeply grateful to Dr. Darpan Saraswat, who has shown immense amount of patience in teaching me techniques in animal surgery. Her incredible amount of perseverance has always motivated my passion for science. My sincere and special thanks to JP. His efforts in teaching techniques, extensive advice all through my project have been very instrumental during the course of my thesis work. He is a true inspiration and has always motivated me by his ideas to be a great researcher. He always cheers everyone up, is a fun person and a great friend.

I would also like to share my sincere thanks to Divyangi and Jahnavi who have always been there for me through the happy and difficult times and providing me a lot of emotional support.

I would also like to thank Dr. Slaughter, Kara Rickicki and Lisa Zander for their support and advice during the masters program.

I am also deeply grateful to my room mates Prajna, Sneha and Sadhana who made life in Buffalo a very cheerful one.

Last but not the least, I would like to thank my family for their endless support and for believing in me and giving all the encouragement and affection I needed.

Table of Contents

Acknowledgments ii
List of Figures vi
List of Tables vii
Abstract viii
1 Introduction 1
1.1 CNS Demyelination and Therapeutic Targets for Remyelination 1
1.2 Animal Models to Study Remyelination 1
1.3 Intracellular and Extracellular Signaling pathways that affect OPC differentiation 2
1.4 Muscarinic Signaling affects OPC differentiation 3
1.5 Significance of Endothelial OPC niche 4
2 Materials and Methods 6
2.1 Animals and Surgeries 6
2.1.1 Surgery- Lysolecithin Injection 6
2.1.2 Surgery-Lipopolysaccharide injection 7
2.1.3 Tissue Fixation 7
2.1.4 Tissue processing/Sectioning 8
2.2 Immunohistochemistry / Immunocytochemistry 9
2.2.1 Eriochrome Cyanine Staining 9
2.2.2 Triton Based Staining for tissue sections 9
2.2.3 Triton Based staining for Cells 11
2.3 Mouse (P7, P14 and Adult) Brain Tissue Dissociation – $CD31^+$ Endothelial Cell Preparation 12
2.3.1 Mouse Brain Tissue Extraction 12
2.3.2 Tissue Processing 12
2.3.3 Flow cytometry Analysis and Sorting 13
2.3.4 Post Sort Endothelial Culture 13
2.4 Human CD140a/PDGFRαR cell preparation 13
2.5 Human $CD31^+$ endothelial cell preparation 14
2.6 Co-culture of human Endothelial Cells and human Oligodendrocyte Progenitor Cells 14
3 Cellular Source of Acetylcholine during Remyelination 16
3.1 Background 16

3.2 Increase in number of cells expressing ChAT during lysoelcithin model of remyelination 17

3.3 Cellular source of ACh during lysoelcithin induced remyelination is neuronal 20

3.4 Increase in cell numbers expressing ChAT during LPS inflammation induced demyelination 25

3.5 Cellular source of ACh in LPS inflammation induced demyelination is predominantly neuronal 28

4 Regulation of ChAT Expression in Developmental Stages of Mice Brain in Uninjured State 33

4.1 Background 33

4.2 ChAT expression in developmental stages of mice brain in uninjured state 33

4.3 Upregulation of mouse endothelial ChAT expression post sort 37

5 Effect of Endothelial Cells on hOPC Proliferation and Differentiation 39

5.1 Background 39

5.2 Human endothelial Cells increase hOPC proliferation in co-culture 39

5.3 Human Endothelial Cells do not affect hOPC differentiation 40

6 Discussion, Conclusion and Future Direction 43

Appendix A: Reagents 47

Appendix B: Detailed Protocols 52

References 55

List of Figures

Figure 1: Lysolecithin Model of remyelination

Figure 2: Generation of ChAT^{BAC}-eGFP transgenic mice

Figure 3: Lysolecithin Induced demyelination on ChAT GFP mice

Figure 4: ChAT expression in 1 dpl lysolecithin focally demyelinated tissue

Figure 5: ChAT expression in 3 dpl lysolecithin focally demyelinated tissue

Figure 6: ChAT expression in 5 dpl lysolecithin focally demyelinated tissue

Figure 7: ChAT expression in 7 dpl lysolecithin focally demyelinated tissue

Figure 8: LPS-inflammation induced demyelination in ChAT GFP mice.

Figure 9: ChAT expression in LPS inflammation induced demyelination at 1 dpl

Figure 10: ChAT expression in LPS inflammation induced demyelination at 3 dpl

Figure 11: ChAT expression in LPS inflammation induced demyelination at 7 dpl

Figure 12: Flow cytometry analysis on developmental stages of mouse brain and fetal human brain

Figure 13: Upregulated ChAT GFP expression in mouse endothelial cells

Figure 14: Effect of human endothelial cells on hOPC proliferation and differentiation.

List of Tables

Table 1: List of antibodies and immunohistochemistry methods

Table 2: List of antibodies and immunocytochemistry methods

Table 3: Summary of ChAT expression in Lysolecithin demyelination and LPS inflammation induced demyelination models

Abstract

Acetylcholine (ACh) plays an important role in inhibiting oligodendrocyte differentiation and remyelination through the activation of muscarinic receptors. However, the cellular source of acetylcholine involved in this signaling has not been established. Using a BAC transgenic ChAT GFP mouse model, we identified neuronal cells as a potential source of acetylcholine following lysolecithin demyelination. We obtained consistent results of neuronal ChAT expression in intraspinal inflammation caused by LPS which modelled inflammation inducing demyelination as observed in MS lesions. However, this does not exclude other non-neuronal sources of ACh released during remyelination. We hypothesized that ACh produced from endothelial cells acts on oligodendrocyte progenitor cells (OPCs) via M1/3 receptor and inhibits oligodendrocyte differentiation. To define the regulation of ChAT expression in intact brain, we performed flow cytometry analysis of ChAT-GFP mouse brain at postnatal day 7, day 14, and adult mice. We observed a very small fraction of endothelial cells expressing detectable ChAT GFP in the uninjured state. Intriguingly, following dissociation, isolated ChAT-GFP negative $CD31^+$ endothelial cells progressively up-regulated GFP post sorting and seeding. This suggests that endothelial ACh expression may be induced by various environmental stimuli. Through co-culture experiments between hOPCs and human endothelial cells, we observed an increase in hOPC proliferation, however, we did not see an effect of endothelial cells on hOPC differentiation. Future experiments will investigate the mechanisms by which endothelial cells may act as potential modulators of hOPC proliferation and provide insight into the interplay between endothelial cells and OPCs in demyelinating diseases like MS.

1 Introduction

1.1 CNS Demyelination and Therapeutic Targets for Remyelination

Oligodendrocyte progenitor cells (OPCs) in the central nervous system (CNS) play a vital role in providing myelin sheath around neuronal axons to achieve efficient signal transduction. CNS demyelination can occur due to genetic abnormalities such as Krabbe Disease) [1], inflammation that affect the glial population such as Multiple, Sclerosis [2] and non-disease related factors such as age and sex [3]. Injury to oligodendrocytes causes damage to the myelin sheath around axons disrupting signal transduction. As a repair process, inflammatory cells such as microglia, astrocytes sense an imbalance in the tissue homeostasis and release important factors that activate OPCs. Following this, OPCs are recruited to the demyelinated regions and undergo differentiation into mature oligodendrocytes. This leads to replenishment of myelin around the axon (remyelination) and thus, regaining function in the demyelinated neuronal segment. When this remyelination process is hindered over a long period of time, it leads to axonal damage and irreversible loss of neurons which progresses a disease state [4].

1.2 Animal Models to Study Remyelination

Several models are used today to depict white matter injury which include, ethidium bromide (EtBr), lysophosphatidylcholine (Lysolecithin). Focal Demyelination models such as the above mentioned examples enable us to look specifically at the region of white matter where demyelination occurs. The process of remyelination happens in a temporal fashion wherein we observe macrophage and microglial infiltration, reactive astrogliosis, axonal injury, OPC proliferation and migration. Hence, this model is

particularly useful as we can understand signaling mechanisms associated with remyelination process at the site of white matter injury [5] **(Figure 1).**

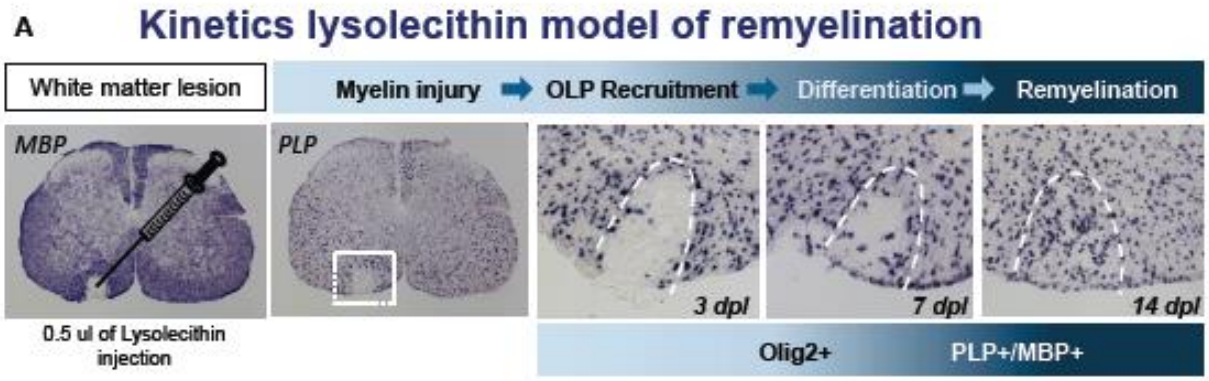

Figure 1: Schematic illustration of lysolecithin causing a white matter injury, followed by time dependent recruitment of OPCs to the site of lesion helping in remyelination after differentiating into mature oligodendrocytes. (Lee et al, 2015)

Other animal models to understand the process of remyelination include treatment of copper chelating compounds such as cuprizone which targets oligodendrocytes and causes subsequent demyelination [6]. The Experimental Autoimmune Encephalomyelitis (EAE) model mimics autoimmune/inflammatory demyelinating disease such as MS [7]. For our experiment, we will be using the lysolecithin based focal demyelination model.

1.3 Intracellular and Extracellular Signaling pathways that affect OPC differentiation

Several research studies aim to identify key intracellular signaling pathways that influence remyelination [8, 9]. For example, research by Tawk et al. demonstrated that activating Wnt signaling by molecules like Wnt1, increases three-fold transcription of myelin genes such as myelin protein zero (MPZ) in OPCs *in vitro* [10]. Similarly, the PI3K/Akt downstream effector, mTOR is necessary for oligodendrocyte maturation and myelination in spinal cord as demonstrated through Cre-lox conditional knockout of mTOR in

oligodendrocytes [11]. These examples illustrate the importance of targeting intracellular signaling pathways to enhance remyelination.

On the extracellular milieu, cholinergic signaling and its function in myelin and action potential propagation have been a major focus of interest since 1950s. Modification of cholinesterase activity has been suggested as early as 1958 by Zinnitz and Hammer as a possible therapeutic for Multiple Sclerosis [12]. Kim et al. in 1972 suggested that ACh receptor expression and AChE activity increased during myelination, but its potential action on glial cells in white matter was unknown [13]. In the recent years, research in this field is of upcoming interest and several drugs such as Clemastine, traditionally an anti-histamine but also known to have anticholinergic effects, has been shown to enhance OPC differentiation [14, 15]. Clemastine fumarate is currently on a Phase 2 Clinical trial as a remyelinating agent in Relapsing Remitting Multiple Sclerosis (RRMS) patients [16]. However, clemastine as a drug has many off target effects and hence, required doses to treat RRMS may cause other deleterious effects [17]. This suggests that, more research focus is required in understanding the cholinergic signaling mechanism associated with OPC maturation and remyelination with perhaps a more receptor specific therapeutic target.

1.4 Muscarinic Signaling affects OPC differentiation

Previous research in our lab has demonstrated that treatment of hOPCs with a muscarinic agonist such as oxotremorine inhibits hOPC differentiation into mature oligodendrocytes in a dose dependent manner [18]. This supports the idea that, acetylcholine activates M1/3 receptor and blocks the OPC maturation during remyelination. To investigate if neuronal ACh delays OPC differentiation, Abiraman et al. conducted a co-culture

experiment with hOPCs and ChAT$^+$ neuronal culture with a muscarinic antagonist (darifenacin). They observed an increase in differentiation of hOPCs compared to matched serum free co-culture conditions. Co-culture conditions treated with acetylcholinesterase inhibitor such as Chlorpyrifos, significantly decreased hOPC differentiation [18]. However, this does not exclude the possibility that there may be other cellular sources of ACh that affect OPC differentiation. Inhibiting this source of ACh could act as a potential therapeutic strategy to enhance the differentiation of OPCs thus leading to faster myelin regeneration. In the sections later, we have shown evidence suggesting mouse brain microvascular endothelial cells as a potential source of ACh and analyzed the possible effect of endothelial ACh on hOPC differentiation.

1.5 Significance of Endothelial OPC niche

The cerebral endothelium interacts with neuronal precursors by trophic signaling to form a neurovascular niche. This interaction helps in proliferation and maintenance of stem-ness in neuronal progenitor cells (NPCs). Similarly, interaction of cerebral endothelium with non-neuronal sources such as astrocytes, pericytes and OPCs help in formation and functioning of BBB. The importance of OPCs to interact with endothelium in providing integrity to BBB has been shown in a recent study by Seo, J.H., et al. where they explain how lack of TGF-β signaling from OPCs can cause disruption to BBB integrity [19]. Leaky BBB can pave way for entry of leukocytes and cause demyelination, tissue damage and axonal dysfunction [20]. The cerebral endothelium and OPCs have a mutual relationship for each other's functioning in terms of trophic signaling. For example, the endothelium releases trophic factors such as FGF and BDNF for the survival and proliferation of OPCs by pathways such as Akt and Src [21]. On the other hand, the OPCs release TGF-β for

maintaining the interaction between pericytes and endothelium in maintaining BBB integrity. More research is yet to be done to identify other trophic factors and associated signaling pathways influencing this oligovascular niche. Another approach to show increase in survival of OPCs by influence of endothelium, has been shown by Ishizak et al. where transplantation of microvascular endothelial cells into demyelinating lesion reduced the lesion size in turn reducing infarct volume [22]. They also hypothesized that inflammation which is usually caused by microglia and macrophages caused apoptosis of OPCs and this can be inhibited by transplantation of brain microvascular endothelial cells.

Thus, from the above examples, we understand that a mutual relationship exists between OPCs and endothelial cells. However, the influence of endothelial cholinergic signaling on OPCs is not well established.

The research in this thesis is based on the following aims:

1) To identify the cellular source of ACh during remyelination through studying the expression of a precursor molecule of ACh; Choline acetyltransferase (ChAT).
2) Elucidate the expression of ChAT and its regulation in adult and developing stages of mice.
3) To understand effect of this cellular source on OPC differentiation and proliferation. To examine the factors that may influence the expression of ChAT and the release of ACh.

2 Materials and Methods

2.1 Animals and Surgeries

2.1.1 Surgery- Lysolecithin Injection

All experiments were performed according to protocols approved by University at Buffalo Institutional Animal Care and Use Committee (IACUC). ChAT^{BAC} eGFP (B6.Cg-Tg(RP23-268L19-EGFP)2Mik/J) mice were obtained from Jackson Laboratories and animals from twenty five - thirty five weeks were used for lysolecithin induced focal demyelination. All surgical instruments were pre-sterilized by autoclaving. Demyelinated spinal cord lesions were generated in the ventrolateral and dorsal white matter. Animals were anesthetized by 1.5-2% isofluorane by inhalation. Animals were given 0.1 mg/kg buprenorphine subcutaneously for analgesia. Paralube was applied on the eyes of the mouse. Toe pinch test was administered to see if animal is sufficiently anesthetized. After shaving the back of the mouse and applying iodine, an incision of about one centimeter (1 cm) was made with scissors. Fascia was trimmed away from either sides of the incision with scissors. Next, using two Dumont 5 forceps, the ligament flava and overlying musculature were removed until the underlying cord is exposed; identified by the milky white color with its central vein running down the middle of the cord. The cord was then tented upward slightly using a pair of mosquito forceps. A 27.5 gauge needle was used to make a small incision into dura to the left of central vein with bevel side up. Using a micromanipulator, a Hamilton syringe needle adjusted to a 70◦ angle was inserted into the spinal cord through the incision until a deflection of the needle was observed. Once, the Hamilton needle is inserted, 0.5 µL of Lysolecithin (1% solution, Sigma) given as 0.2 + 0.2 + 0.1 µL was injected and allowed about 1 minute for solution to diffuse for each injection. The

micromanipulator knob close to Hamilton was adjusted to “20” and another 0.5 µL of lysolecithin was injected as explained previously. This creates a ventral white matter lesion. For a dorsal lesion, the needle was completely removed from the cord and re-inserted such that the needle tip lies just inside the dura and another 0.5 µL of lysolecithin was injected. About 1 minute was given for the lysolecithin to diffuse and the needle was removed. A single 6-0 suture was placed above the lesion site anchored in the white ligament in either side of the spinal cord. Three to five sutures were placed externally. Another dose of buprenorphine (0.1 mg/kg) was given subcutaneously. The animal was then placed in a warm chamber before returning to the home cage. Respiratory rate, pain reflex, and mucous membrane color were observed for every animal.

2.1.2 Surgery-Lipopolysaccharide injection

Steps in 2.1.1 were followed for LPS injections at a dose of 100 ng/µL and a total volume of 1.5 µL for dorsal and ventral white matter lesions.

2.1.3 Tissue Fixation

We have used 4 time points for the lysolecithin focal demyelination (1 dpl, 3 dpl, 5 dpl and 7 dpl) and 3 time points for LPS injections (1 dpl, 3 dpl, 7 dpl). Animals were given 80 mg/kg Pentobarbital Sodium injected intraperitoneal (IP) as an anesthetic before the perfusion process. Toe pinch test was administered to see if animal is sufficiently anesthetized. Animal was then placed on a Styrofoam lid. 18 gauge needles were used for holding the mice on the Styrofoam. The peristaltic pump was set up and was connected to a 26G needle. The sternum of the mouse was located and using scissors, the skin and ribs over the thoracic cavity was cut off. The chest flap was carefully pinned to one side, so that the heart is clearly visible. The saline needle was inserted into the left

ventricle and was clamped in place with hemostat. Using nippers, the right atrium of the heart was cut. The timer for saline was set for 10 minutes for saline to pass through. After that, the valve was switched to 4 % PFA for 15 minutes.

Before removing the spinal cord tissue, firstly the internal suture was located. Using scalpel blades, spinal cord tissue along with its musculature was obtained using No. 11 scalpel blades. This tissue was then fixed further overnight in 4% PFA.

2.1.4 Tissue processing/Sectioning

Following day, the spinal cord tissue was then placed in 1x PBS in 4◦C overnight. The 1xPBS was replaced with 6% sucrose the next day and 8 hours later, the solution was replaced with 15% sucrose and left overnight.

The spinal cord tissue was extracted using forceps and scissors. A sharpie mark was placed at the point where the needle mark was inserted in the spinal cord. Cords were then embedded and frozen on Optimal Cutting Temperature (O.C.T) medium in 2-methylbutane over dry ice. Blocks were stored in -80◦C until ready for sectioning. Blocks were trimmed in a cryostat until a lesion was observed with DAPI staining. Lesions were identified by an increased density of $DAPI^+$ cells showing infiltration of cells into the lesion site (infiltration of cells for lysolecithin and LPS is seen after 3 dpl). Four 16 µm-thick sections were collected per slide in series of 10 slides until lesions were no longer observed. Slides were stored in -80◦C until further staining experiments.

2.2 Immunohistochemistry / Immunocytochemistry

2.2.1 Eriochrome Cyanine Staining

Slides were removed from -80◦C and allowed to reach room temperature. Slides were dehydrated through 70%, 95% and 100% ethanol and were subsequently rehydrated through 95%, 70% and distilled water for 5 minute intervals. Sections were then stained using the eriochrome cyanine (Appendix A) for 15 minutes. Slides were placed in differentiation solution (Appendix A) for ten-second duration and placed in water. This was repeated four times to achieve proper color depth. Slides were washed 5 minutes in distilled water, dehydrated in 5 minutes intervals in 70%, 95% and 100% ethanol followed by 5 minute steps in pure xylene. Coverslips were mounted using OpticMount Xylene (Mercedes Medical) and allowed to seal overnight.

2.2.2 Triton Based Staining for tissue sections

Slides were brought to room temperature from -80◦C. Slides were washed three times for 5 minutes in 1xPBS plus thimerosol. (Appendix A) and blocked for 1 hour using Triton Brain Block (Appendix A). Sections were stained with primary antibody diluted in Brain SD (Appendix A) overnight at 4◦C.

Antibody	Cell type marker	Catalog No.	Antigen Retrieval	Permeabilization	Blocking	Primary Antibody Concentration
CD31	Endothelial Cells	BD Pharmingen 550274	Nil	1% Triton (30 min)	Triton Brain Block (1hr)	1:200
PDGFRβ	Pericytes	Abcam Ab32570	Nil	1% Triton (30 min)	Triton Brain Block (1 hr)	1:500
GFAP	Astrocytes	Sigma G3893	Nil	1% Triton (30 min)	Triton Brain Block 1 hr) and Mouse on Mouse block (1 hr)	1:400
Olig2	Oligodendrocytes	Millipore AB9610MI	Nil	1% Triton (30 min)	Triton Brain Block (1 hr)	1:500
Iba1	Microglia	Wako Chemicals USA 019-19741	Nil	1% Triton (30 min)	Triton Brain Block (1 hr)	1:1000
NF	Axonal neurofilament	SMI312R (Biolegend) SMI-312R Covance Research Products, Inc SMI-311R	Methanol and slides kept at -20◦ C (1 hr)	1% Triton (30 min)	Triton Brain Block (1 hr) and Mouse on Mouse block (1 hr)	1:1000
APP	Amyloid precursor protein (injured axon)	ThermoFisher Scientific (Invitrogen) 512700	Nil	1% Triton (30 min)	Triton Brain Block (1 hr)	1:300
GFP	Green fluorescent protein	Abcam Ab13970	Nil	1% Triton (30 min)	Triton Brain Block (1 hr)	1:300

Table 1: List of antibodies and immunohistochemistry methods

Following day, slides were washed three times with PBS plus thimerosol. Slides were blocked with Brain Block (Appendix A) for 1 hour at room temperature. Sections were then stained with appropriate secondary antibodies diluted in Brain SD for 1 hour at room temperature. Sections were washed three times with PBS with thimerosol. These sections were counterstained with DAPI (1:5000) for 3 minutes and again washed three times with PBS/T. The slides were mounted with ProLong Gold, sealed with nail polish and were left overnight to dry.

2.2.3 Triton Based staining for Cells

2.2.3.1 O4 Live cell Staining

Cells were live stained with O4 mouse hybridoma antibody at 1:20 for 30 minutes. The cells were fixed with 4% Paraformaldeyde. The plate can be stored in 4◦C until ready to be stained. The cells were gently washed three times with PBS/T. Further, they were treated with 5% Goat serum in HBSS(+) (Blocking) for an hour. Then the cells were secondary stained for O4 using the appropriate secondary (Goat anti Ms IgM 594).

2.2.3.2 Fixed Cell Staining

Fixed plate was brought to room temperature. The plates were gently washed three times with PBS/T. The cells were permeabilized with 0.1% Triton Permeabilization Buffer for 30 minutes (Appendix A). The cells were then blocked with 0.01% Triton Blocking Buffer (Appendix A) for an hour. These were then incubated with the respective primary antibody in Triton Standard Diluent Buffer (Appendix A) overnight in 4◦C. The following day, the cells were washed three times with PBS/T. The cells were again blocked with 0.01% Triton Blocking buffer for an hour. Further, the cells were treated with the appropriate secondary in Triton Standard Diluent for an hour. The cells were then counter stained with DAPI.

Antibody	**Cell type marker**	**Catalog No.**	**Permeabilization**	**Blocking**	**Primary Antibody Concentration**
Olig 2	Premature Oligodendrocytes	Millipore AB9610MI	0.1% Triton	0.01% Triton Blocking Buffer	1:800
vWF	Endothelial Cells	AbCam ab6994	0.1% Triton	0.01% Triton Blocking Buffer	1:500

Table 2: List of antibodies and immunocytochemistry methods

2.3 Mouse (P7, P14 and Adult) Brain Tissue Dissociation – CD31^{+} Endothelial Cell Preparation

2.3.1 Mouse Brain Tissue Extraction

The animals were administered Sodium Pentobarbital as an anesthetic through an intraperitoneal injection at a dose of 80mg/kg. The animal was administered a toe pinch test to see if it was sufficiently anesthetized. Cervical dislocation was performed as a secondary method to confirm death. A number 10 Scalpel blade was used to cut through the neck. Using scissors, the skin covering the skull was incised. Meninges that surround the skull were also removed. Using nippers, the lateral posterior ridges on each side of the skull were cut. A scissors was used to cut through the skull from rostral to caudal end without going deep into the brain tissue. Using forceps, the skull was removed and brain was scooped out using a spatula.

2.3.2 Tissue Processing

The brains were removed and stored in chilled HBSS(+) for further processing. For an adult mouse tissue, the corpus callosum and cerebellum were removed to minimize myelin debris. The tissue was washed at least three times in HBSS(+). Clots on the brain were removed. The brain tissue was minced using #10 scalpel blades. 1.5ml aliquots of minced tissue were collected using disposal sterile bulb pipette into a 15 ml conical.

Papain (Appendix A) was used to digest the tissue. DNAse was added to avoid clumping of cells together. Further the tissue was then triturated with decreasing radii of fire polished glass Pasteur pipettes. The tissue was then re-suspended in cold Sort Wash Buffer (Appendix A). The tissue was processed for myelin removal using myelin removal beads (Miltenyi Biotech, Catalog No. 130-096-733) as per manufacturer's instructions

(For detailed protocol Refer Appendix B). The cells were then taken for flow cytometry analysis and sorting.

2.3.3 Flow cytometry Analysis and Sorting

The cells were stained with CD31 PE conjugated fluorophore (Fisher Scientific, BDB561073) and analysed for ChAT expression and $CD31^+$ endothelial cells. The cells were sorted for ChAT GFP^- $CD31^+$ cells using BD FACS Aria Fusion Cell Sorter.

2.3.4 Post Sort Endothelial Culture

Sorted $CD31^+$ endothelial cells from Section 2.3.3 were seeded in a complete Endothelial Growth Medium (EGM) (Appendix A). Prior to seeding, the wells were coated with bovine collagen 1 (Fisher Scientific, Catalog No. A1064401) coated wells at 50µg/ml in glacial acetic acid.

2.4 Human CD140a/PDGFRαR cell preparation

Fetal brain samples (17-22 week gestational age) were obtained from patients who consented to tissue use under protocols approved by University at Buffalo Research Subjects Institutional Review Board. Forebrain tissue was minced and dissociated using papain and DNAse as previously described [23]. Magnetic Sorting of CD140a positive cells was performed as described [24]. The cells were seeded on poly-L-ornithine and laminin coated plates and were maintained in neural differentiation (ND) media (Appendix A) [18]. Cells were maintained in progenitor state in presence of growth factors 20ng/ml PDGF-AA (Peprotech) and 5 ng/ml of NT-3 (Peprotech).

2.5 Human $CD31^+$ endothelial cell preparation

Fetal brain samples (17-22 week gestational age) were obtained from patients who consented to tissue use under protocols approved by University at Buffalo Research Subjects Institutional Review Board. Forebrain tissue was minced and dissociated using papain and DNAse as previously described [23]. About 80 million cells were seeded on a 100 mm suspension dish. The cells were recovered after 2 days. 10 ml of media from the top was removed without disturbing the cells. 100 µL of DNAse was added to the dish. The dish was washed and cells were collected in a 50 ml conical. The dish was washed with HBSS(-) three times. The supernatant was removed completely and the cells were re-suspended in 2.5 ml of cold Sort Wash Buffer (30 million per ml). The cells were counted and stained for CD31 (BD Pharmingen BD560983) mouse anti-human as per manufacturer's instructions. 100K cells (100 µL) was kept aside as an unstained sample. After staining, the cells were kept in the nutator for 15 minutes in 4◦C. Cold Sort Wash Buffer was added to the tubes and spun for 7 minutes at 4 clicks. The cells were again re-suspended at 30 million/ml and were filtered with blue cap FACS tubes. The cells were taken for flow cytometry analysis and collection tubes were filled with EGM media after cell sorting. After sorting, the $CD31^+GFP^-$ endothelial cells were seeded on bovine collagen coated wells with complete EGM media.

2.6 Co-culture of human Endothelial Cells and human Oligodendrocyte Progenitor Cells

12 wells of a 48-well plate were coated with Poly-O-Laminin. The wells were washed with HBSS(+) and on Day 0, human Endothelial Cells were seeded onto 8 wells at a density of 70k/ml with complete EGM (Endothelial Growth Media). After 8 hours, all 12 wells were changed to the following different media conditions

1) ND media with PDGF-AA and NT-3

2) ND media without PDGF-AA and NT-3

3) ND media with PDGF-AA, NT-3, Vascular Endothelial Growth Factor (VEGF), Insulin Growth Factor (IGF), Hydrocortisone and Ascorbic Acid

4) ND Media without PDGF-AA and NT-3 with Vascular Endothelial Growth Factor (VEGF), Insulin Growth Factor (IGF), Hydrocortisone and Ascorbic Acid

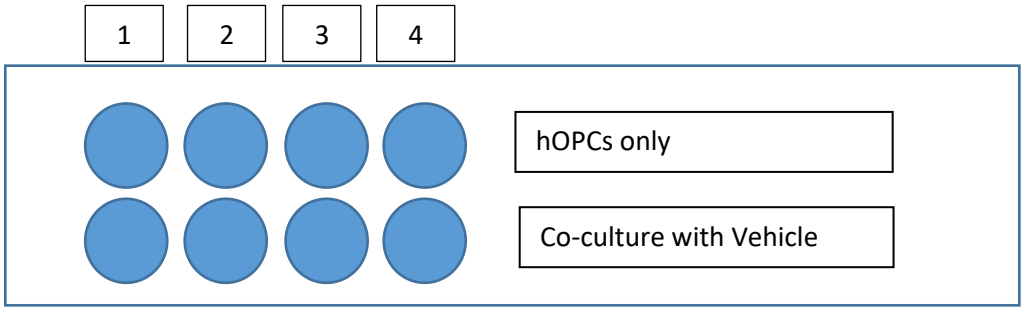

On the following day (Day 1), hOPCs were seeded at 50k/ml on all the wells with respective media conditions as stated in the figure above. We left the cultures on for Day 2 and Day 3 without any media change. On Day 4, a pulse of EdU at 10 µM was given to the cells 8 hours prior to fixation, to observe proliferation. The cells were live stained for O4 and were fixed after 30 minutes with 4% Paraformaldeyde. The cells were further stained for EdU as per manufacturer's instructions (C10641, Invitrogen). Secondary staining for O4 and EdU were performed. Cells were also stained with Olig2. The images were processed and the percentage proliferation and differentiation were obtained by counting the $O4^+$ or EdU positive cells. The $O4^+$ cells were counted into simple and complex based on the number of branches present (less than 3 were considered simple and greater than or equal to 3 were considered as complex).

3 Cellular Source of Acetylcholine during Remyelination

3.1 Background

Cholinergic neurons are traditionally the major players of synthesis of ACh and mediates neurotransmission by means of receptors such as nAChRs and mAChRs. More recently, there are a number of research studies elucidating non-neuronal sources of ACh such as epithelial [25], immune cells such as T,B cells and macrophages [26], endothelial cells [27]. Non-neuronal ACh source has shown to play important functions in signal transduction as demonstrated in epithelial keratinocytes where ACh triggers Ca^{2+} influx further affecting downstream pathways such as Ras, Raf, MEK, ERG CamKII etc. [28]. Other functions of non-neuronal ACh include promoting proliferation and differentiation of epidermal cells [29].

In our study, we wanted to identify cellular sources of ACh during remyelination. To achieve this, we utilized a $ChAT^{BAC}$-eGFP transgenic mouse model [30]. This mouse model is particularly useful as we observe ChAT GFP expression in central and peripheral cholinergic neurons, including cell bodies and processes of the somatic sensory and motor neurons as well as post-ganglionic parasympathetic process innervating target organs. This model has also shown evidence of ChAT in non-neuronal cell types such as epithelial cells and T-lymphocytes in intestine and lung thus, invigorating our interest to use this model.

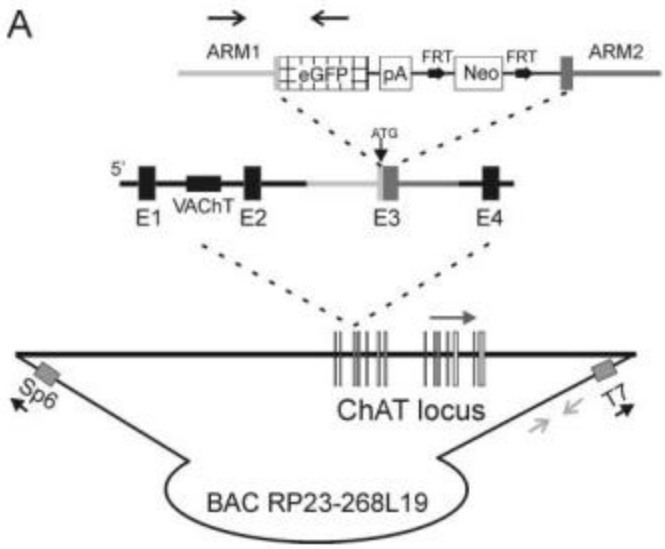

Figure 2: Generation of ChAT^{BAC}-eGFP transgenic mice. eGFP inserted into the third exon to replace the start codon of ChAT gene (Adapted from Tallini et al. [30]).

To study ChAT expression at different stages of remyelination, we utilized the lysolecithin based focal demyelination model. Lysolecithin is a myelin solubilizing agent which particularly targets the oligodendrocytes. We observe infiltration of inflammatory cells and recruitment of oligodendrocytes to the site of lesion in a time dependent manner depicting the stages of remyelination [5, 31]. This model is thus particularly useful for our study to look at ChAT expression in cell types during remyelination (Refer to Material and Methods for detailed Lysolecithin injection).

3.2 Increase in number of cells expressing ChAT during lysoelcithin model of remyelination

We observed the ChAT expression at 4 different time points (1, 3, 5, 7 days post lesion (dpl)). The animal was euthanized and spinal cord tissue was processed (Refer Material and Methods). We identified ventrolateral lesions through solochrome cyanine staining (**Figure 3A, 3D, 3G and 3J**). As is expected, we observed hyper-cellularity at 3 dpl, 5 dpl and 7 dpl demarcated by the DAPI staining **(Figure 3B, 3E, 3H and 3K)** suggesting the

infiltration of cells to the site of lesion temporally. We observed an increase in the number of ChAT expressing cells from 1 dpl to 3 dpl (**Figure 3C and 3F**) and a sudden increase in the ChAT expressing cells at 7 dpl (**Figure 3L**). The increasing number of ChAT expressing cells may indicate an increase in the release of ACh during remyelination.

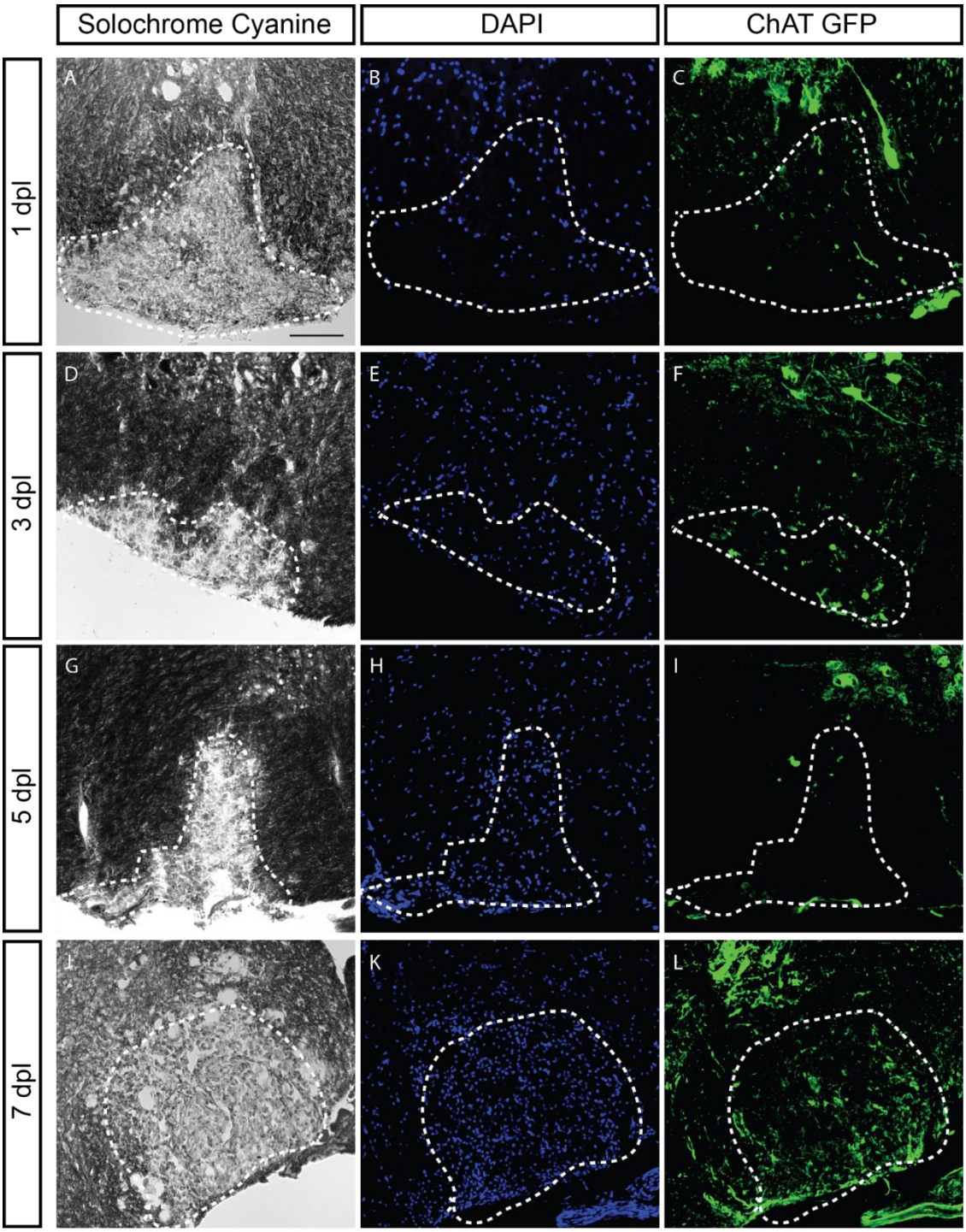

Figure 3: Lysolecithin induced demyelination in ChAT GFP mice. Presence of a ventrolateral lesion (dotted line) caused by lysolecithin at (A) 1 dpl, (D) 3 dpl, (G) 5 dpl, (J) 7 dpl, depicted by solochrome cyanine. Increasing recruitment of cells to the point of lesion depicted by $DAPI^+$ cells at (B) 1 dpl (E) 3 dpl (H) 5 dpl (K) 7 dpl). Increasing number of ChAT expressing cells to the point of lesion depicted by GFP^+ cells (C) 1 dpl (F) 3 dpl (I) 5 dpl (L) 7 dpl). Scale 100 µm

3.3 Cellular source of ACh during lysoelcithin induced remyelination is neuronal

ChAT expression in different cell types was observed by performing immunohistochemistry. We labelled cell types that included, endothelial, pericytes, astrocytes, microglia, oligodendrocytes and injured axons (Refer to Materials and Methods for detailed protocol and antibody dilutions). We used confocal microscopy at a 60x magnification and performed orthogonal projection of the images, to confirm ChAT expression in these cell types. For better quality images, we used deconvolution by Autoquant software.

As expected, we observed co-localization between NF^+APP^+ ChAT GFP^+ cells and also NF^+ ChAT GFP^+ cells inside lesion suggesting that neurons express ChAT and release ACh during remyelination. The co-localization of NF+ APP+ ChAT GFP+ cells show that several injured axons also release ACh during remyelination. We also identified occasional punctate ChAT GFP staining in $GFAP^+$ astrocytes but didn't see a clear co-localization of ChAT expression in nuclei of astrocytes. We observed $Iba1^+$ cells phagocytosing $ChAT^+$ cells but similarly did not visualize a clear co-localization of uniform ChAT expression among nuclei of microglial cells. No ChAT GFP expression was observed in either $CD31^+$ endothelial cells or the $PDGFR\beta^+$ pericytes that are closely associated with endothelial cells. Similarly, no expression of ChAT was observed in $Olig2^+$ premature oligodendrocytes. All these data were consistent across different time points and no change in expression of ChAT amongst these cells was observed.

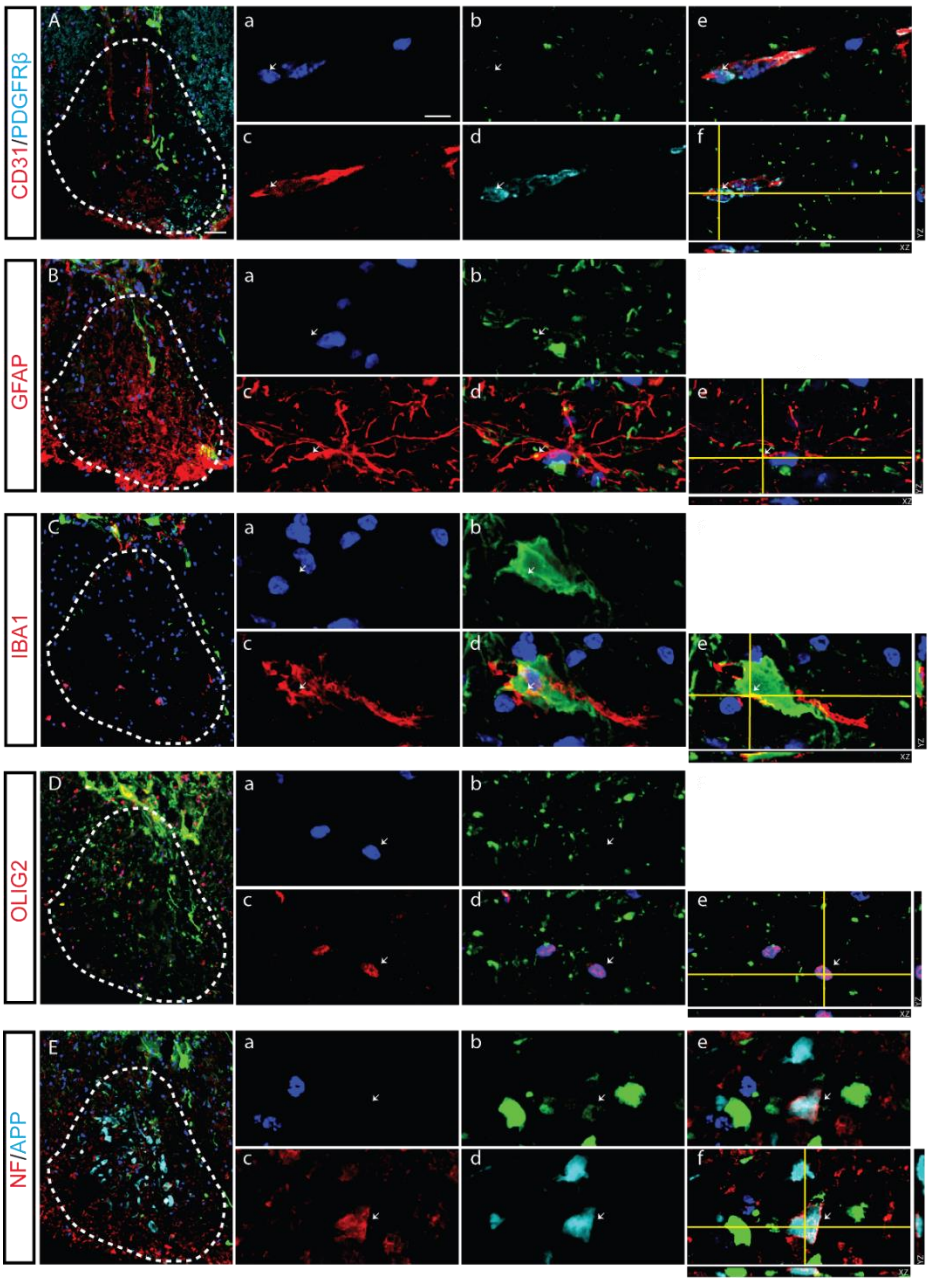

Figure 4: ChAT expression in 1 dpl lysolecithin focally demyelinated tissues. A, Sections were stained with CD31 labelling endothelial cells and PDGFRβ labelling pericytes (10x). A(a) DAPI, A(b) ChAT GFP, A(c) CD31, A(d) PDGFRβ, A(e) Composite, A(f) orthogonal projection does not show co-localization of ChAT GFP in endothelial or pericytes. B, Sections were stained with GFAP labelling astrocytes (10x), B(a) DAPI, B(b) ChAT GFP, B(c) GFAP, B(d) Composite, B(e) orthogonal projection does not show co-localization of ChAT GFP in astrocytes. C, Sections were stained with Iba1 labelling microglia (10x), C(a) DAPI, C(b) ChAT GFP, C(c) Iba1, C(d) Composite, C(e) orthogonal projection does not show co-localization of ChAT GFP in microglia. D, Sections were stained with Olig2 labelling oligodendrocytes (10x), D(a) DAPI, D(b) ChAT GFP, D(c) Olig2, D(d) Composite, D(e) orthogonal projection does not show co-localization of ChAT GFP in oligodendrocytes. E, Sections were stained with NF labelling axons and APP labelling injured axons (10x). E(a) DAPI, E(b) ChAT GFP, E(c) NF, E(d) APP, E(e) Composite, E(f) orthogonal projection shows close apposition seen between NF, APP and ChAT. Scale (10x) 50 µm, (60x) 10 µm

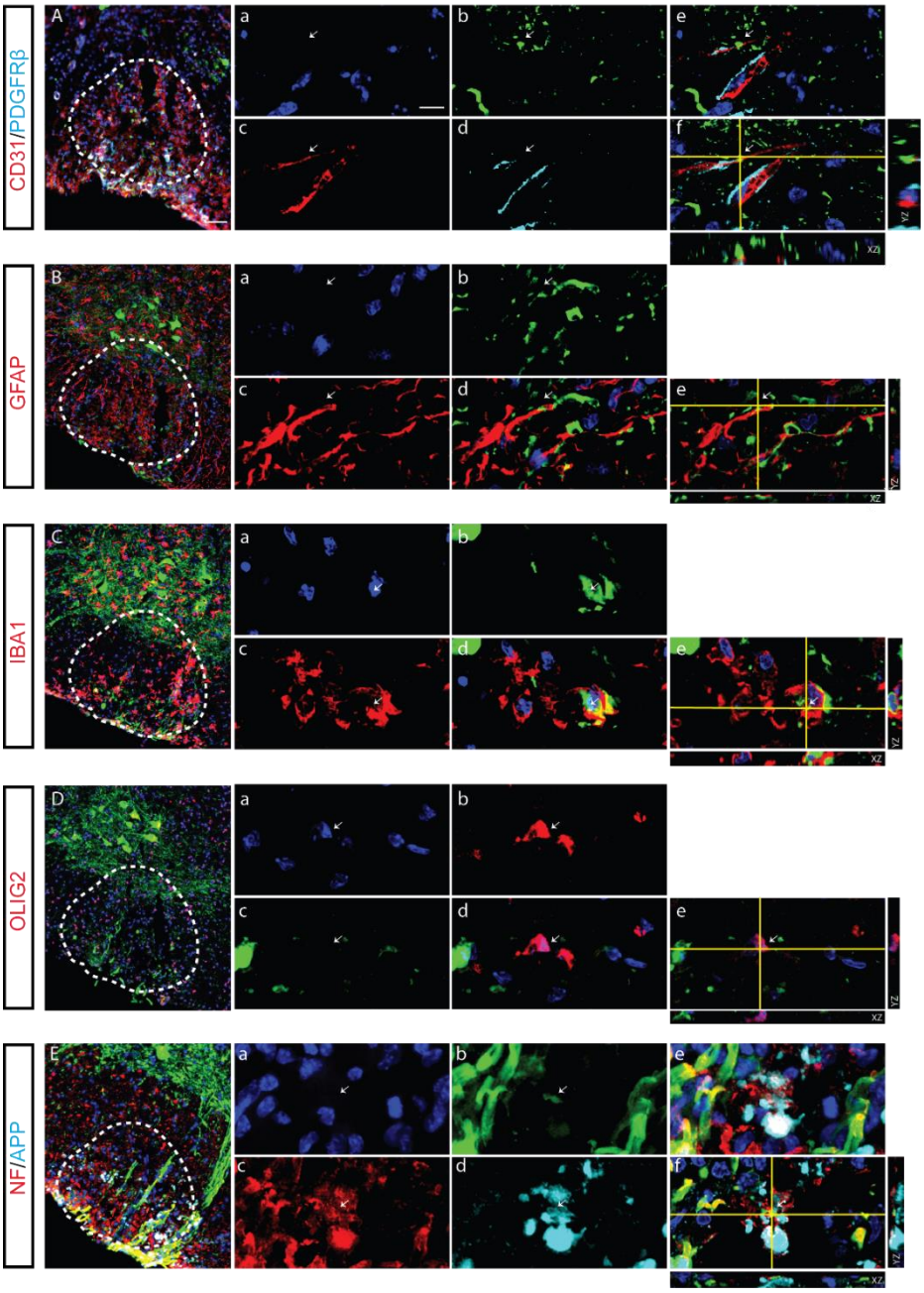

Figure 5: ChAT expression in 3 dpl lysolecithin focally demyelinated tissues. A, Sections were stained with CD31 labelling endothelial cells and PDGFRβ labelling pericytes (10x). A(a) DAPI, A(b) ChAT GFP, A(c) CD31, A(d) PDGFRβ, A(e) Composite, A(f) orthogonal projection does not show co-localization of ChAT GFP in endothelial or pericytes. B, Sections were stained with GFAP labelling astrocytes (10x), B(a) DAPI, B(b) ChAT GFP, B(c) GFAP, B(d) Composite, B(e) orthogonal projection does not show co-localization of ChAT GFP in astrocytes. C, Sections were stained with Iba1 labelling microglia (10x), C(a) DAPI, C(b) ChAT GFP, C(c) Iba1, C(d) Composite, C(e) orthogonal projection does not show co-localization of ChAT GFP in microglia. D, Sections were stained with Olig2 labelling oligodendrocytes (10x), D(a) DAPI, D(b) ChAT GFP, D(c) Olig2, D(d) Composite, D(e) orthogonal projection does not show co-localization of ChAT GFP in oligodendrocytes. E, Sections were stained with NF labelling axons and APP labelling injured axons (10x). E(a) DAPI, E(b) ChAT GFP, E(c) NF, E(d) APP, E(e) Composite, E(f) orthogonal projection shows close apposition seen between NF, APP and ChAT. Scale (10x) 50 µm, (60x) 10 µm

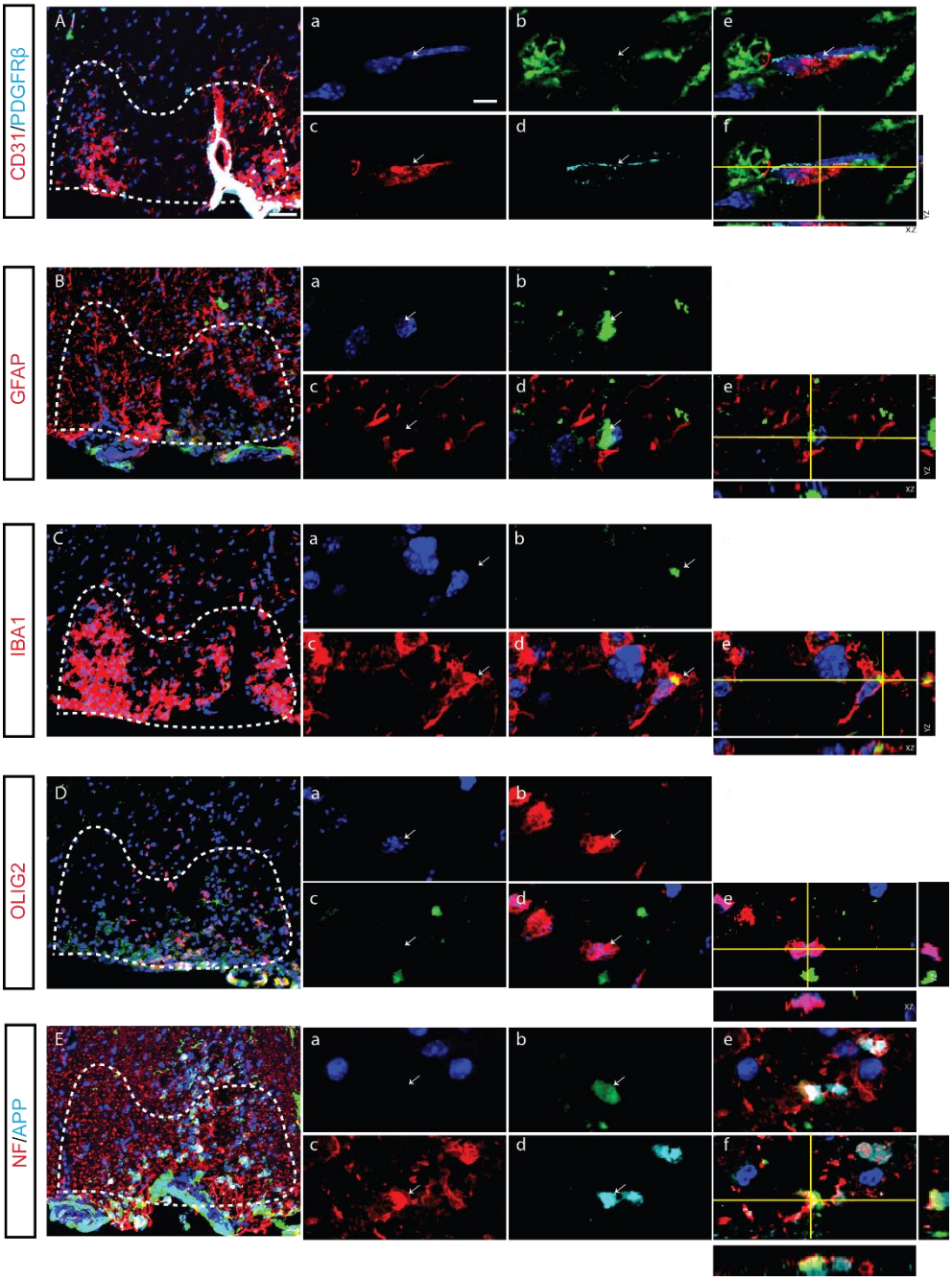

Figure 6: ChAT expression in 5 dpl lysolecithin focally demyelinated tissues. A, Sections were stained with CD31 labelling endothelial cells and PDGFRβ labelling pericytes (10x). A(a) DAPI, A(b) ChAT GFP, A(c) CD31, A(d) PDGFRβ, A(e) Composite, A(f) orthogonal projection does not show co-localization of ChAT GFP in endothelial or pericytes. B, Sections were stained with GFAP labelling astrocytes (10x), B(a) DAPI, B(b) ChAT GFP, B(c) GFAP, B(d) Composite, B(e) orthogonal projection does not show co-localization of ChAT GFP in astrocytes. C, Sections were stained with Iba1 labelling microglia (10x), C(a) DAPI, C(b) ChAT GFP, C(c) Iba1, C(d) Composite, C(e) orthogonal projection does not show co-localization of ChAT GFP in microglia. D, Sections were stained with Olig2 labelling oligodendrocytes (10x), D(a) DAPI, D(b) ChAT GFP, D(c) Olig2, D(d) Composite, D(e) orthogonal projection does not show co-localization of ChAT GFP in oligodendrocytes. E, Sections were stained with NF labelling axons and APP labelling injured axons (10x). E(a) DAPI, E(b) ChAT GFP, E(c) NF, E(d) APP, E(e) Composite, E(f) orthogonal projection shows close apposition seen between NF, APP and ChAT. Scale (10x) 50 µm, (60x) 10 µm

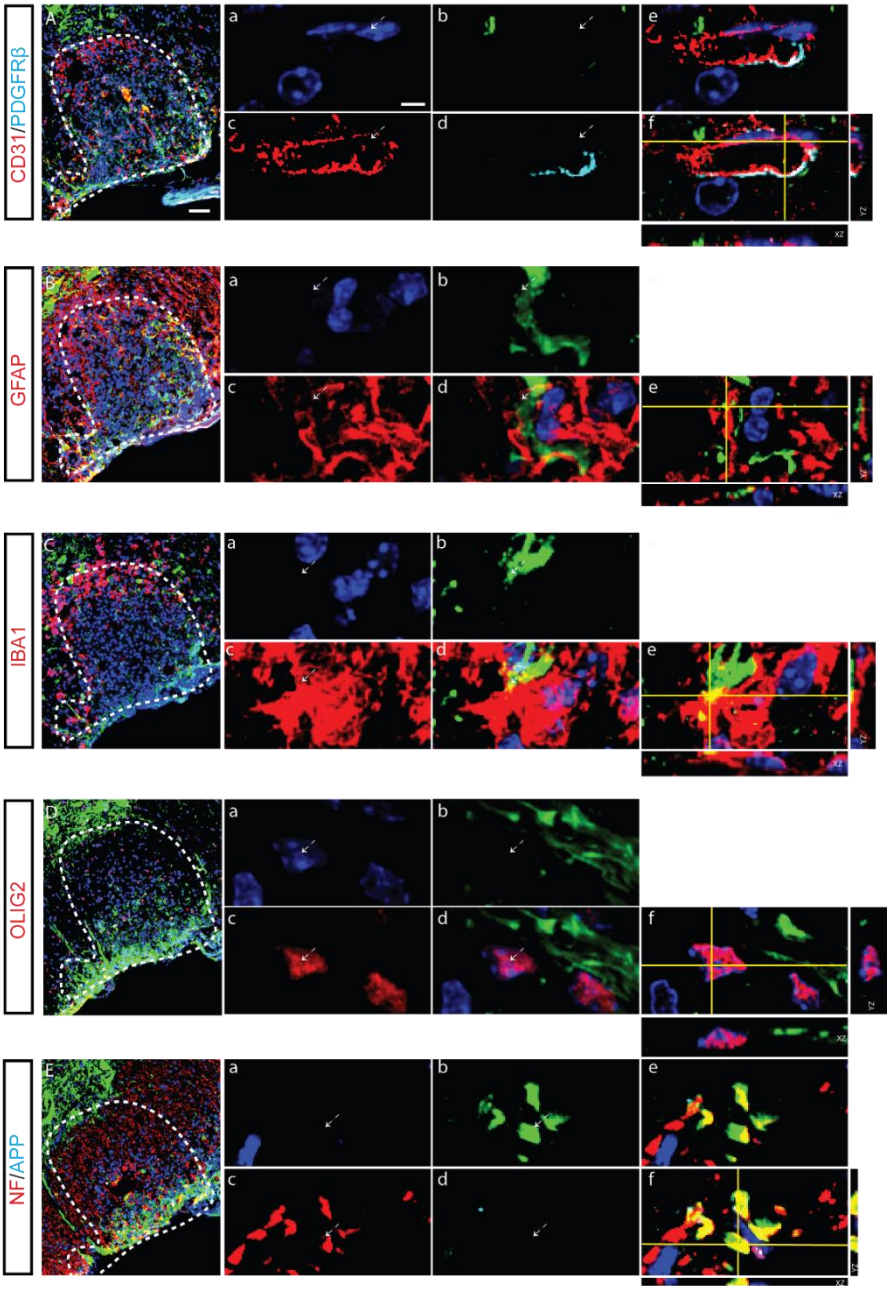

Figure 7: ChAT expression in 7 dpl lysolecithin focally demyelinated tissues. A, Sections were stained with CD31 labelling endothelial cells and PDGFRβ labelling pericytes (10x). A(a) DAPI, A(b) ChAT GFP, A(c) CD31, A(d) PDGFRβ, A(e) Composite, A(f) orthogonal projection does not show co-localization of ChAT GFP in endothelial or pericytes. B, Sections were stained with GFAP labelling astrocytes (10x), B(a) DAPI, B(b) ChAT GFP, B(c) GFAP, B(d) Composite, B(e) orthogonal projection does not show co-localization of ChAT GFP in astrocytes. C, Sections were stained with Iba1 labelling microglia (10x), C(a) DAPI, C(b) ChAT GFP, C(c) Iba1, C(d) Composite, C(e) orthogonal projection does not show co-localization of ChAT GFP in microglia. D, Sections were stained with Olig2 labelling oligodendrocytes (10x), D(a) DAPI, D(b) ChAT GFP, D(c) Olig2, D(d) Composite, D(e) orthogonal projection does not show co-localization of ChAT GFP in oligodendrocytes. E, Sections were stained with NF labelling axons and APP labelling injured axons (10x). E(a) DAPI, E(b) ChAT GFP, E(c) NF, E(d) APP, E(e) Composite, E(f) orthogonal projection shows close apposition seen between NF and ChAT but no APP. Scale (10x) 50 µm, (60x) 10 µm

3.4 Increase in cell numbers expressing ChAT during LPS inflammation induced demyelination

Demyelinating diseases such as Multiple Sclerosis (MS) are associated with a pathologic hallmark of inflammatory lesions with axonal damage and astrogliosis. Inflammation in MS has been hypothesized to be caused due to disturbance of Blood Brain Barrier (BBB); lymphocytes through their interaction of integrins with cell adhesion molecules on endothelial cells enables easy access through the BBB and thus triggers inflammation [32]. Other pathologic factors of inflammation include T cells recruiting macrophages to initiate lesion formation by presenting antigens [33, 34].

Intraspinal injection of Lipopolysaccharide (LPS) has been previously used to induce an innate inflammatory response which triggers hypoxic like conditions in the white matter thus giving rise to energy insufficiency. This further leads to death of vulnerable cells such as oligodendrocytes eventually causing lesion and subsequent prominent demyelination at 7 days. We used this model to simulate inflammation that gives rise to a prominent demyelinated lesion [35, 36] as seen in MS patients (Pattern 3 mechanism of lesion formation). ChAT expression in cell types of this condition may be useful for us to understand its role in remyelination.

We injected LPS intraspinally at 100ng/µL into mouse spinal cord similar to the Lysolecithin injection (Refer Materials Methods). Animals were euthanized and tissues were processed after 1, 3 and 7 days post injection. Immunohistochemistry was done to visualize ChAT expression in cell types. We observed no demyelination for the 1 dpl animals and a slight infiltration of microglial cells towards the lateral side of the spinal cord suggesting action of LPS at this region at 1 dpl (**Figure 9C**)**.** We visualize increasing

hypercellularity from 1 dpl **(Figure 8E)** to 3 dpl **(Figure 8H)** and 7 dpl **(Figure K)** and progressive demyelinating lesion through these time points **(Figure 8 (D,G,J))** which were consistent with the results obtained by Felts, P. A. et al. [35]. We observe increasing number of ChAT expressing cells in the area of inflammation **(Figure 8 (F,I,L))** compared to uninjured mouse spinal cord (**Figure 8C**). This indicates a potential increase in release of ACh due to action of LPS inducing inflammation in the lesion area.

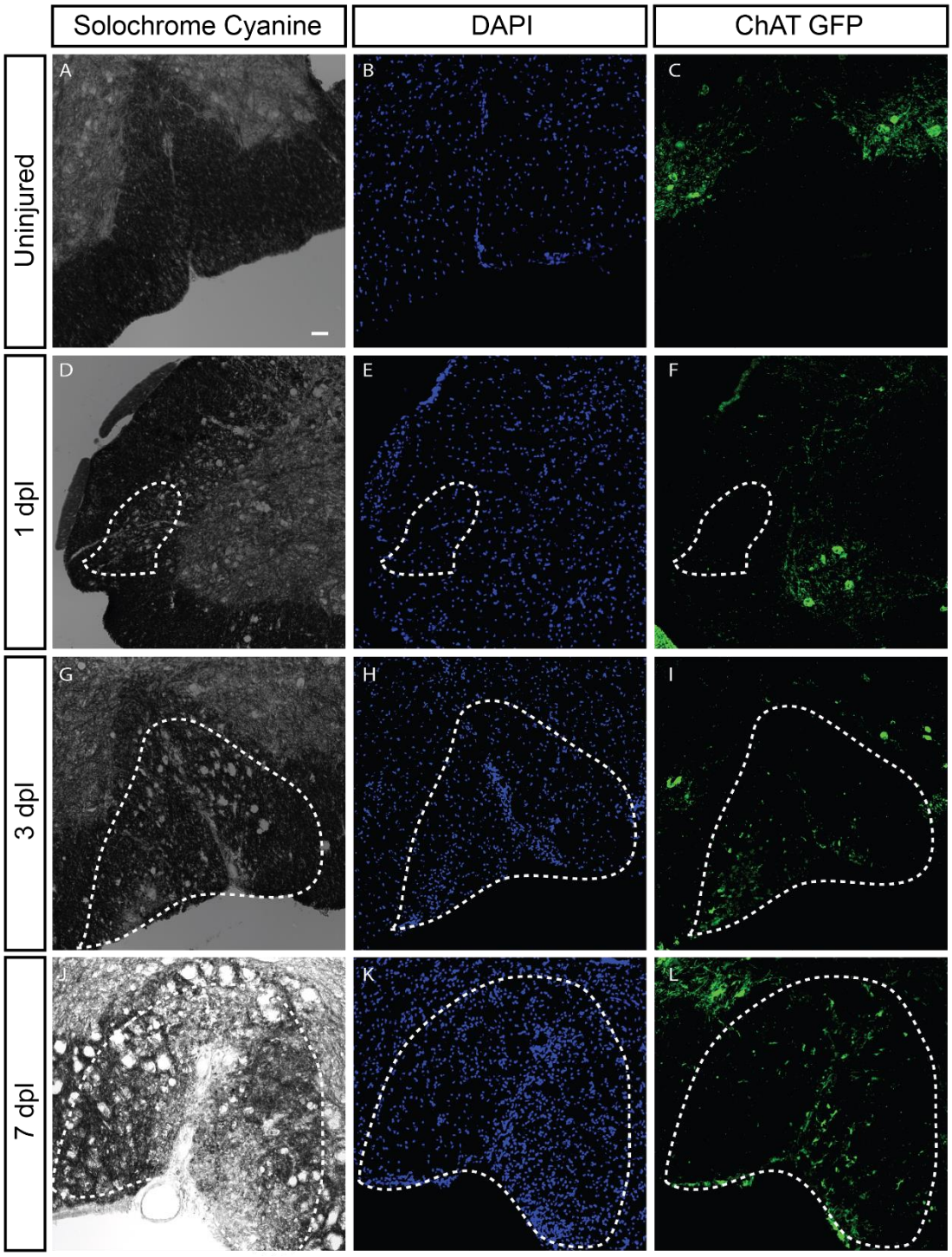

Figure 8: LPS-inflammation induced demyelination in ChAT GFP mice. A, No presence of lesion in control ChAT GFP mouse B, DAPI staining in uninjured mouse C, ChAT GFP in uninjured mouse. Presence of a lateral (1 dpl), ventral lesion (3, 7 dpl) (dotted line) caused by LPS at (D) 1 dpl, (G) 3 dpl, (J) 7 dpl, depicted by solochrome cyanine. Increasing recruitment of cells to the point of lesion depicted by $DAPI^+$ cells at (E) 1 dpl (H) 3 dpl (K) 7 dpl). Increasing number of ChAT expressing cells to the point of lesion depicted by GFP^+ cells (F) 1 dpl (I) 3 dpl (L) 7 dpl). Scale 50 µm

3.5 Cellular source of ACh in LPS inflammation induced demyelination is predominantly neuronal

Immunohistochemistry was performed to visualize ChAT expression in other cell types. We performed 60x confocal imaging and processed orthogonal projections to visualize ChAT expression in these cells. Similar to the lysolecithin experiment, we observed a number of $ChAT^+$ NF^+ cells suggesting ChAT expression in neuronal axons in the lesion area. However, we didn't observe many NF+APP+ ChAT GFP+ cells suggesting absence of injured axons expressing ChAT. We observed occasional punctate $ChAT^+$ staining in $GFAP^+$ astrocytes but did not observe a uniform distribution of ChAT in the nucleus of the GFAP+ cell. We observed $Iba1^+$ microglia phagocytosing $ChAT^+$ cells but we do not observe clear co-localization of $ChAT^+Iba1^+$ cells. No co-localization was observed between ChAT and $Olig2^+$ oligodendrocytes. All these data indicate neuronal source of ACh in these LPS injected conditions which was consistent with our lysolecithin demyelination experiment.

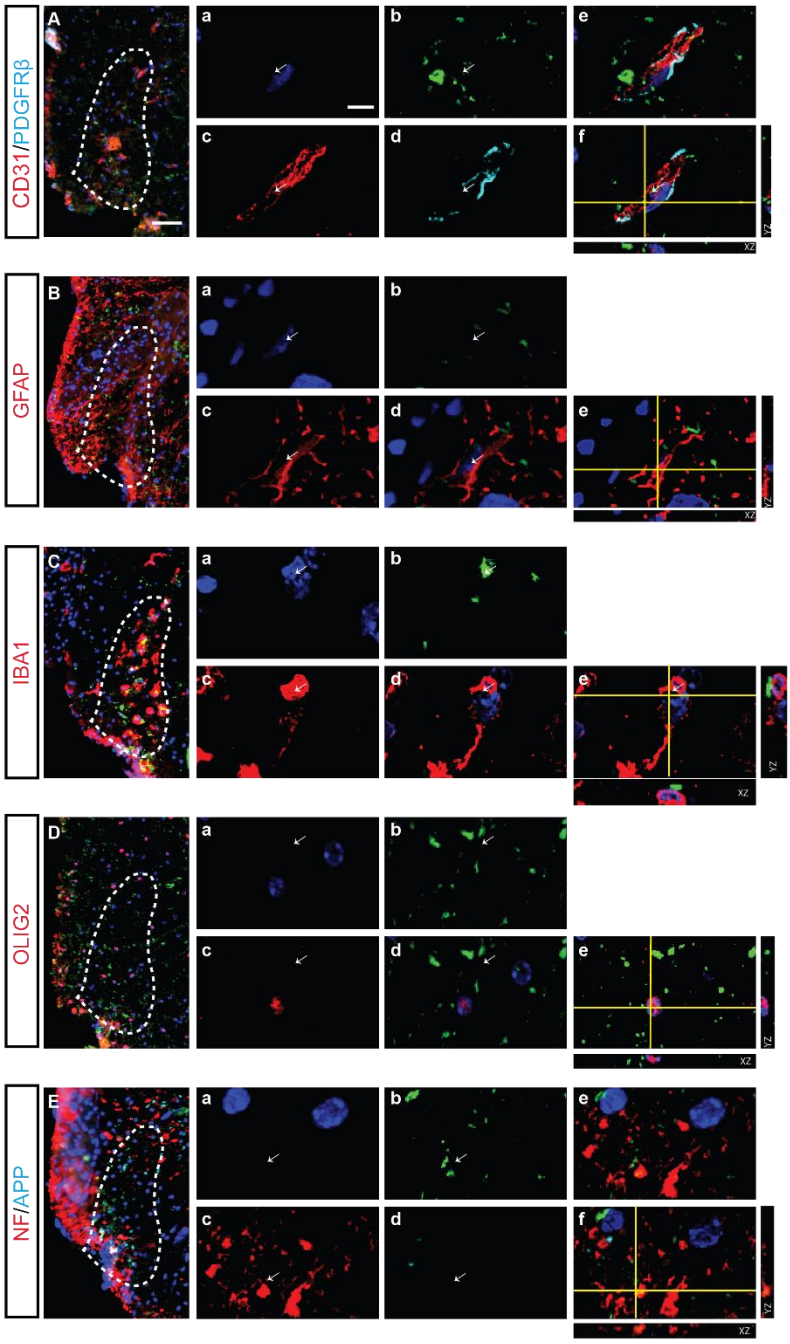

Figure 9: ChAT expression in LPS inflammation induced demyelination at 1 dpl. A, Sections were stained with CD31 labelling endothelial cells and PDGFRβ labelling pericytes (10x). A(a) DAPI, A(b) ChAT GFP, A(c) CD31, A(d) PDGFRβ, A(e) Composite, A(f) orthogonal projection does not show co-localization of ChAT GFP in endothelial or pericytes. B, Sections were stained with GFAP labelling astrocytes (10x), B(a) DAPI, B(b) ChAT GFP, B(c) GFAP, B(d) Composite, B(e) orthogonal projection does not show co-localization of ChAT GFP in astrocytes. C, Sections were stained with Iba1 labelling microglia (10x), C(a) DAPI, C(b) ChAT GFP, C(c) Iba1, C(d) Composite, C(e) orthogonal projection does not show co-localization of ChAT GFP in microglia. D, Sections were stained with Olig2 labelling oligodendrocytes (10x), D(a) DAPI, D(b) ChAT GFP, D(c) Olig2, D(d) Composite, D(e) orthogonal projection does not show co-localization of ChAT GFP in oligodendrocytes. E, Sections were stained with NF labelling axons and APP labelling injured axons (10x). E(a) DAPI, E(b) ChAT GFP, E(c) NF, E(d) APP, E(e) Composite, E(f) orthogonal projection shows close apposition seen between NF and ChAT but no APP. Scale (10x) 50 µm, (60x) 10 µm

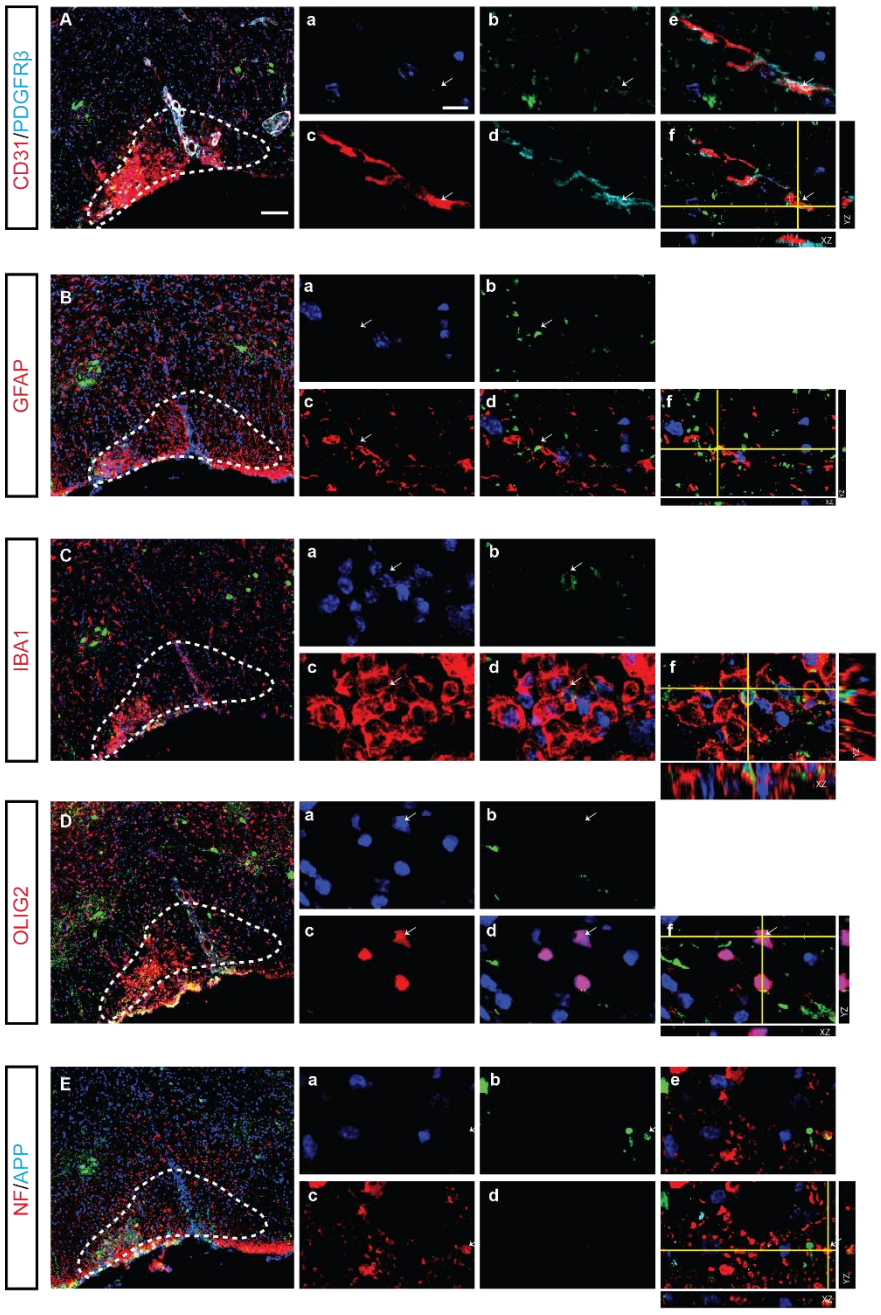

Figure 10: ChAT expression in LPS inflammation induced demyelination at 3 dpl. A, Sections were stained with CD31 labelling endothelial cells and PDGFRβ labelling pericytes (10x). A(a) DAPI, A(b) ChAT GFP, A(c) CD31, A(d) PDGFRβ, A(e) Composite, A(f) orthogonal projection does not show co-localization of ChAT GFP in endothelial or pericytes. B, Sections were stained with GFAP labelling astrocytes (10x), B(a) DAPI, B(b) ChAT GFP, B(c) GFAP, B(d) Composite, B(e) orthogonal projection does not show co-localization of ChAT GFP in astrocytes. C, Sections were stained with Iba1 labelling microglia (10x), C(a) DAPI, C(b) ChAT GFP, C(c) Iba1, C(d) Composite, C(e) orthogonal projection does not show co-localization of ChAT GFP in microglia. D, Sections were stained with Olig2 labelling oligodendrocytes (10x), D(a) DAPI, D(b) ChAT GFP, D(c) Olig2, D(d) Composite, D(e) orthogonal projection does not show co-localization of ChAT GFP in oligodendrocytes. E, Sections were stained with NF labelling axons and APP labelling injured axons (10x). E(a) DAPI, E(b) ChAT GFP, E(c) NF, E(d) APP, E(e) Composite, E(f) orthogonal projection shows close apposition seen between NF and ChAT but no APP. Scale (10x) 50 µm, (60x) 10 µm

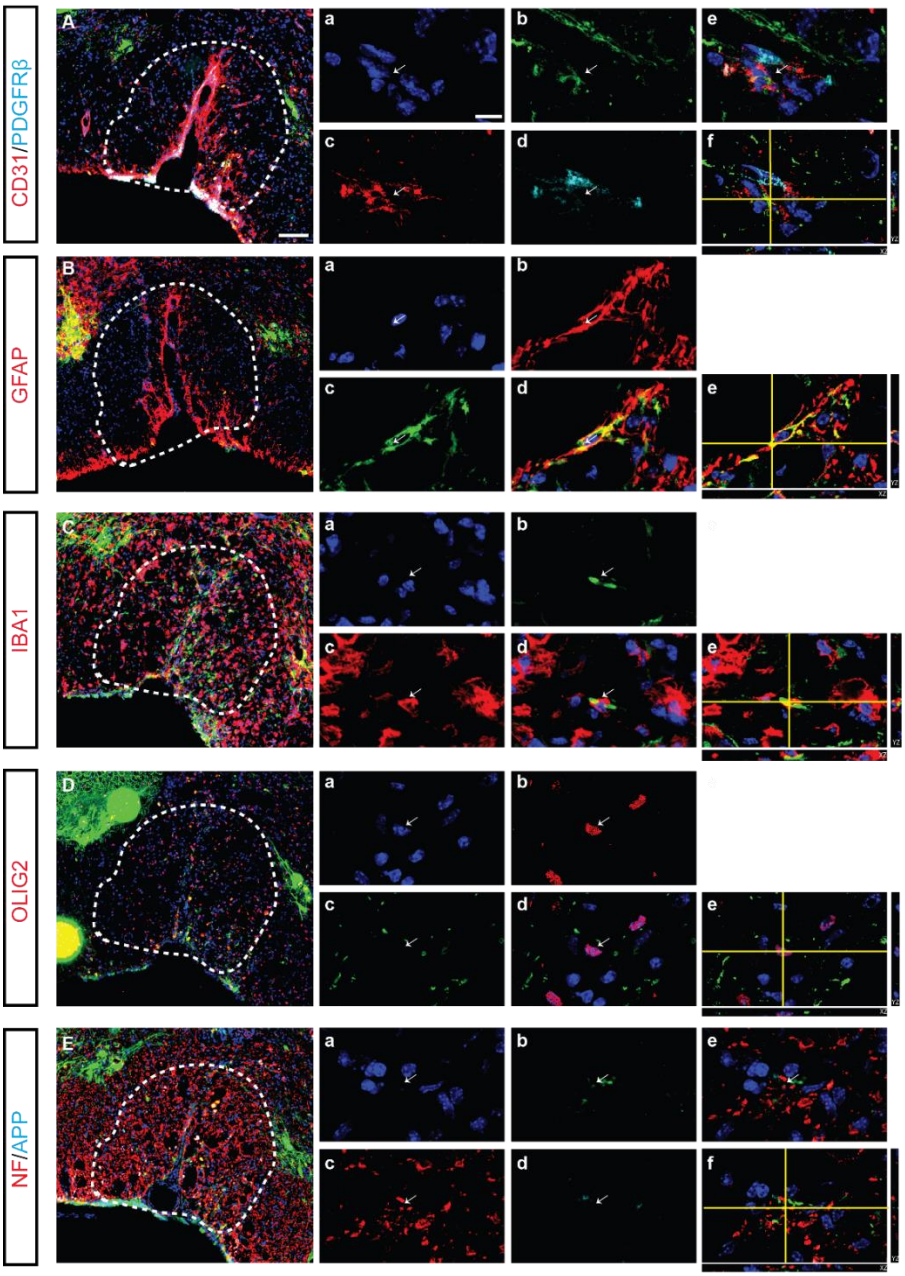

Figure 11: ChAT expression in LPS inflammation induced demyelination at 7 dpl. A, Sections were stained with CD31 labelling endothelial cells and PDGFRβ labelling pericytes (10x). A(a) DAPI, A(b) ChAT GFP, A(c) CD31, A(d) PDGFRβ, A(e) Composite, A(f) orthogonal projection does not show co-localization of ChAT GFP in endothelial or pericytes. B, Sections were stained with GFAP labelling astrocytes (10x), B(a) DAPI, B(b) ChAT GFP, B(c) GFAP, B(d) Composite, B(e) orthogonal projection does not show co-localization of ChAT GFP in astrocytes. C, Sections were stained with Iba1 labelling microglia (10x), C(a) DAPI, C(b) ChAT GFP, C(c) Iba1, C(d) Composite, C(e) orthogonal projection does not show co-localization of ChAT GFP in microglia. D, Sections were stained with Olig2 labelling oligodendrocytes (10x), D(a) DAPI, D(b) ChAT GFP, D(c) Olig2, D(d) Composite, D(e) orthogonal projection does not show co-localization of ChAT GFP in oligodendrocytes. E, Sections were stained with NF labelling axons and APP labelling injured axons (10x). E(a) DAPI, E(b) ChAT GFP, E(c) NF, E(d) APP, E(e) Composite, E(f) orthogonal projection shows close apposition seen between NF and ChAT but no APP. Scale (10x) 50 µm, (60x) 10 µm

	ChAT Expression						
	Lysolecithin				Lipopolysaccharide (LPS)		
Cell Type	**1 dpl**	**3 dpl**	**5 dpl**	**7 dpl**	**1 dpl**	**3 dpl**	**7 dpl**
Endothelial Cells	-	-	-	-	-	-	-
Pericyte	-	-	-	-	-	-	-
Astrocytes	-	-	-	-	-	-	+
Microglia	-	-	-	-	-	-	-
Oligodendrocytes	-	-	-	-	-	-	-
neuron (axon)	+	+	+	+	+	+	+
injured axons	+	+	+	-	-	-	-

Table 3: Summary of ChAT expression in Lysolecithin demyelination and LPS inflammation induced demyelination models

4 Regulation of ChAT Expression in Developmental Stages of Mice Brain in Uninjured State

4.1 Background

Several *in vitro* and *in vivo* studies previously have shown that ChAT enzyme activity can be modulated by several important growth factors in the neurotrophin family including, NGF, BDNF, NT-3, NT-4/NT-5 [37], cytokines [38] and hormones [39]. Recent research studies have also elucidated role of differential ChAT expression levels in pathological conditions in-vivo using transgenic mice models [40]. However, most of these studies have focused predominantly to understand factors regulating neuronal ChAT expression. However, factors that regulate non-neuronal ChAT expression have not been elucidated so far and is a field that needs further research focus. In the upcoming sections, we have elucidated the role of one such non-neuronal source of ACh; endothelial cells. We further elucidate factors that may possibly regulate this expression and its implication towards hOPC proliferation and differentiation.

4.2 ChAT expression in developmental stages of mice brain in uninjured state

In the previous chapter, we looked at ChAT expression in different cell types post demyelination and concluded that neuronal cells are the major ChAT expressing cells during remyelination. Examples from 4.1 suggest that several growth factors, cytokines affect neuronal ChAT expression. We have seen several examples suggesting non-neuronal ChAT expression and its potential functional role (Section 3.1). However, factors affecting non-neuronal ChAT have not been elucidated so far.

To understand this, we first needed to know the basal ChAT expression levels present in the mouse brain. Thus, we extracted cells from ChAT GFP mouse brain from P7, P14 and Adult (35 week) through papain dissociation (Refer Materials and Methods) and performed flow cytometry analysis to observe the population of cells expressing ChAT at different developmental stages. We observed 0.32% of brain cell population expressing ChAT in P7 (**Figure 12 D**) and 0.21% in P14 (**Figure 12 F**) mouse brain. We observed 1.3% of brain cell population expressing ChAT in an adult ChAT GFP mouse (**Figure 12 H**).

ChAT expression in Brain Endothelial cells is close to null

Haberberger, R. V., et al. demonstrated ChAT mRNA expression in endothelial cells from pulmonary vasculature. This suggests that endothelial cells may serve as an endogenous source of ACh [41]. Action of ACh on endothelial cells is known to cause vasorelaxant effects on the underlying smooth muscle cell [42]. Endothelial cells are known to regulate vasoactivity by releasing vasorelaxant factors such as Nitric oxide (NO), prostaglandins and endothelium dependent hyperpolarization factor (EDHF). Additionally another research group Wilson et al. demonstrated flow mediated non-vesicular release of ACh from endothelial cells through organic cation transporters (OCT). The endogenous source of ACh acts as an autocrine signaling molecule and binds to muscarinic receptors present on endothelial cells, triggering Ca^{2+} release from endothelial internal stores which in turn triggers release of vasorelaxant factors such as NO [43].

Even though, in the previous chapter we have shown that, endothelial cells don't express ChAT on focally demyelinated mice spinal cord. We wanted to observe if there were other factors such as shear stress that may influence endothelial ChAT expression.

In order to test this, we performed flow cytometry analysis selecting for endothelial cells by a CD31 PE conjugated antibody. We observed a very minimal population of endothelial cells expressing ChAT (0.02% in P7, 0.01% in P14, 0.01% in adult ChAT GFP mouse) in the uninjured state **(Figure 12 D, F, H).** However, this does not exclude the possibility of other factors that may trigger ChAT expression such as inflammation, hypoxia or shear stress etc.

We also did flow cytometry analysis on fetal human brain and observed 0.35% of brain cell population to be CD31+ endothelial **(Figure 12 J).** We sorted for human endothelial cells which were utilized for co-culture experiments explained in the next chapter.

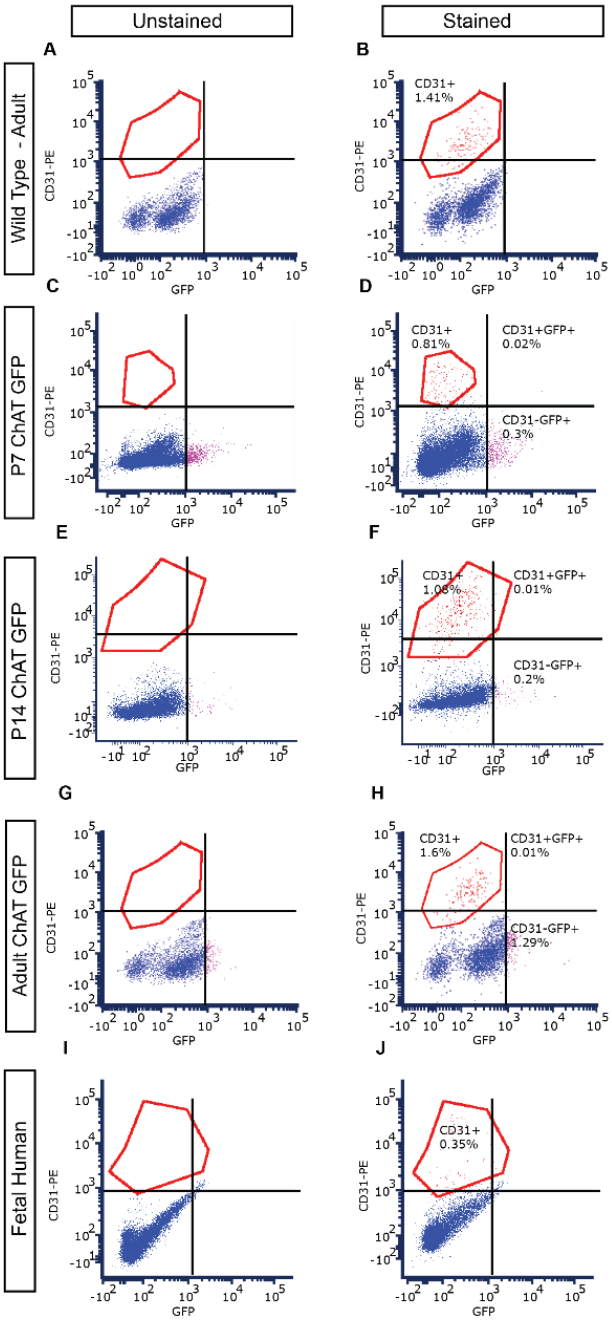

Figure 12: Flow Cytometry Analysis on developmental stages of mouse brain and fetal human brain. **A**, Unstained Wild Type (non ChAT GFP) mouse. **B**, Stained Wild Type mouse-1.41% $CD31^+$ endothelial cells. **C**, P7 Unstained ChAT GFP mouse, **D**, P7 Stained ChAT GFP mouse- 0.3% ChAT GFP^+ cells 0.8% $CD31^+$ endothelial cells, 0.02% $CD31^+GFP^+$. **E**, P14 Unstained ChAT GFP mouse, **F**, P14 Stained ChAT GFP mouse 0.2% ChAT GFP^+ cells 1.08% $CD31^+$ endothelial cells, 0.01% $CD31^+GFP^+$. **G**, Adult Unstained ChAT GFP mouse **H**, Adult Stained ChAT GFP mouse 1.29% ChAT GFP^+ cells 1.6% $CD31^+$ endothelial cells, 0.01% $CD31^+GFP^+$. **I**, Fetal Human Brain Unstained, **J**, Fetal Human Stained 0.35% $CD31^+$ endothelial cells.

4.3 Upregulation of mouse endothelial ChAT expression post sort

We sorted for CD31+ endothelial cells that were GFP^- by Fluorescence Associated Cell Sorting (FACS) and cultured them *in vitro*. We did not observe ChAT expression among these sorted cells immediately after seeding. Intriguingly, we observed progressive upregulation of ChAT expression amongst these endothelial cells 5 days **(Figure 13 E)**, 7 days post **(Figure 13 F)** and 1 month (Passage 3) post sorting **(Figure 13 H)**.

These data indicate that, mouse brain microvascular endothelial cells are capable of expressing ChAT *in vitro* and may possibly be upregulated due to environmental factors. We validated the presence of endothelial cells using an alternate endothelial cell marker, von Willebrand factor (vWF) and obtained a 98% pure population of endothelial cells by 3 passages **(Figure 13 G, J)**. We also validated human endothelial cells using vWF antibody staining **(Figure I, L).**

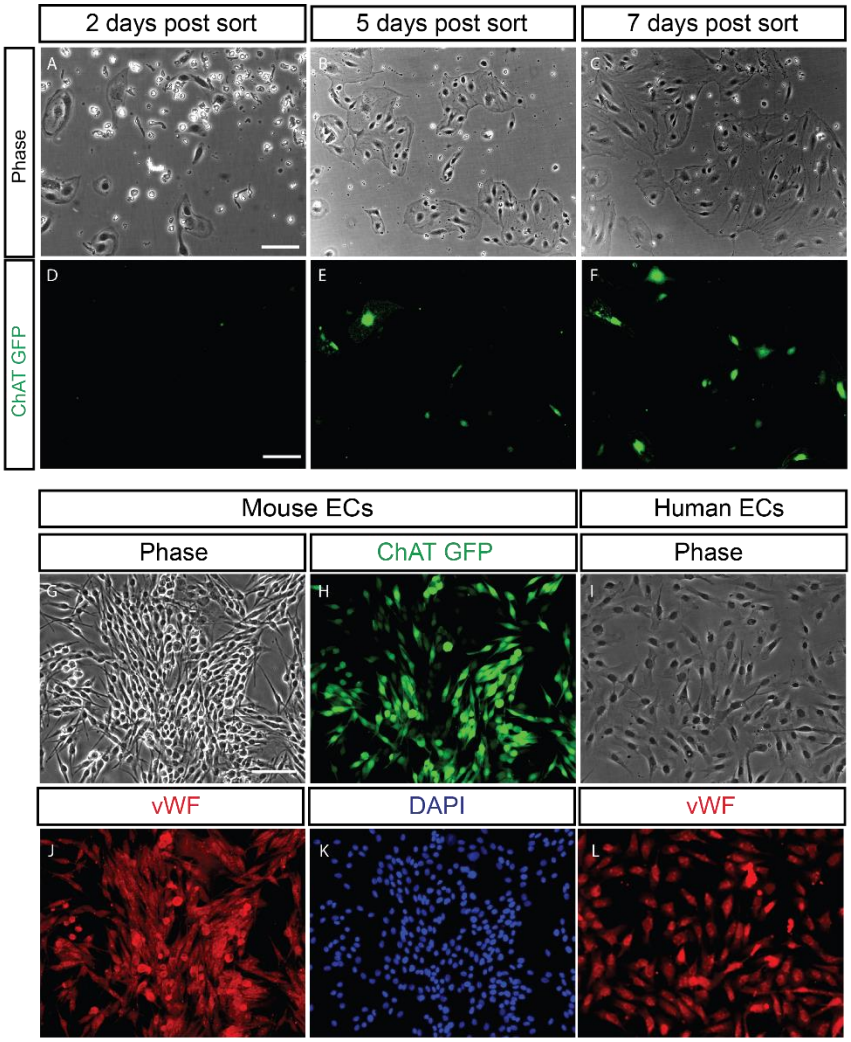

Figure 13: Upregulated ChAT GFP expression in mouse endothelial cells. A, Endothelial cells 2 days post sort **B**, Endothelial cells 5 days post sort **C**, Endothelial cells 7 days post sort **D**, no ChAT GFP expression observed 2 days post sort **E**, ChAT GFP expression observed among endothelial cells at 5 days post sort **F**, upregulated ChAT GFP expression observed among endothelial cells at 7 days post sort **G**, Endothelial cells after a month post sort **H**, 60-70% endothelial cells express ChAT 1 month post sort **J**, vWF staining confirms sorted cells as endothelial cells **K**, DAPI staining of mouse endothelial cells. **I**, human endothelial cells post sorting **L**, vWF staining confirms sorted cells as endothelial cells. Scale: A-F 50µm G-L 100µm

5 Effect of Endothelial Cells on hOPC Proliferation and Differentiation

5.1 Background

Many research studies emphasize the importance of vascular niche and its functional relationship with neuronal precursor cells; microvascular brain endothelial cells has been shown to help in self renewal of Neural Stem Cells (NSCs) and inhibit its differentiation to enhance neuronal production [44]. Transplanted endothelial cells has also shown to induce increased proliferation and survival in injury induced NSCs [45]. Recently, there is growing interest in understanding vascular niche with several other non-neuronal cell types of CNS such as OPCs. A more recent paper by Tsai et al. suggested that OPCs rely on vasculature to migrate from progenitor domains to target site during developing embryonic nervous system [46]. A follow up study to this research suggested that clustering of OPCs to endothelium were initially observed and they eventually migrate to the site of lesion in Wnt dependent matter. Dysfunctionality in this signaling, hinders the separation of OPCs from vasculature, inhibiting its differentiation. This causes clustering feature of OPCs as observed in MS lesion tissue [47]. Above examples show importance of vasculature for hOPC migration during developing nervous system.

5.2 Human endothelial Cells increase hOPC proliferation in co-culture

Several research studies have shown a bidirectional communication between OPCs and vasculature that accomplishes functions such as maintenance of BBB integrity [19], migration [48] survival and proliferation of OPCs. We wanted to understand the effect of

endothelial cells on hOPC proliferation. To accomplish this goal, we performed a co-culture experiment wherein, hOPCs are seeded on a bed of human endothelial cells.

We used 4 different media conditions (with and without PDGF-AA, NT-3, VEGF and IGF) while performing the co-culture experiment in order to avoid differences in proliferation which may be influenced by growth factors in media. PDGF-AA and NT-3 are growth factors that help maintain hOPCs in progenitor state. It has been well established previously that that these growth factors help in proliferation of hOPCs [49] and thus we observe increase in hOPC proliferation in the presence of PDGF-AA and NT-3. On the contrary, in the absence of these factors, we observe increased differentiation of hOPCs.

We used a mono-culture of hOPCs as a control to compare the effect of human endothelial cells on proliferation of hOPCs in the co-culture condition. We observed that, in the presence of human endothelial cells, hOPC proliferation significantly increased compared to the matched monoculture condition irrespective of presence or absence of VEGF and IGF **(Figure 14 G)**. This was consistent with the data obtained by Arai et al. where a similar experiment was conducted between rat OPCs and human endothelial cells [21].

5.3 Human Endothelial Cells do not affect hOPC differentiation

As we observed in Chapter 4, that murine endothelial cells post sort, expressed ChAT progressively, we hypothesized that, human endothelial cells may also express ChAT and may be a potential source of ACh. Thus, we wanted to test if the endothelial release of ACh may have an effect on differentiation of hOPCs. If this held true, we also wanted to find whether this effect may be muscarinic signaling dependent.

From our data, we observe that, compared to matched mono-culture hOPC condition, there is no effect of endothelial cells on hOPC differentiation **(Figure 14 L)**. This effect may suggest two different interpretations. It is possible that human endothelial cells may not express ChAT and thus may not be capable of releasing ACh which could be the reason why we don't see effect of ACh on hOPC differentiation. There may be a species specific differences associated with the expression of ChAT which may explain ChAT expression in mouse endothelial cells but may not necessarily be the case for human endothelial cells.

Secondly, it is possible that there may be presence of Acetylcholine esterases which may degrade ACh released by endothelial cells before it interacted with the muscarinic receptor on hOPCs.

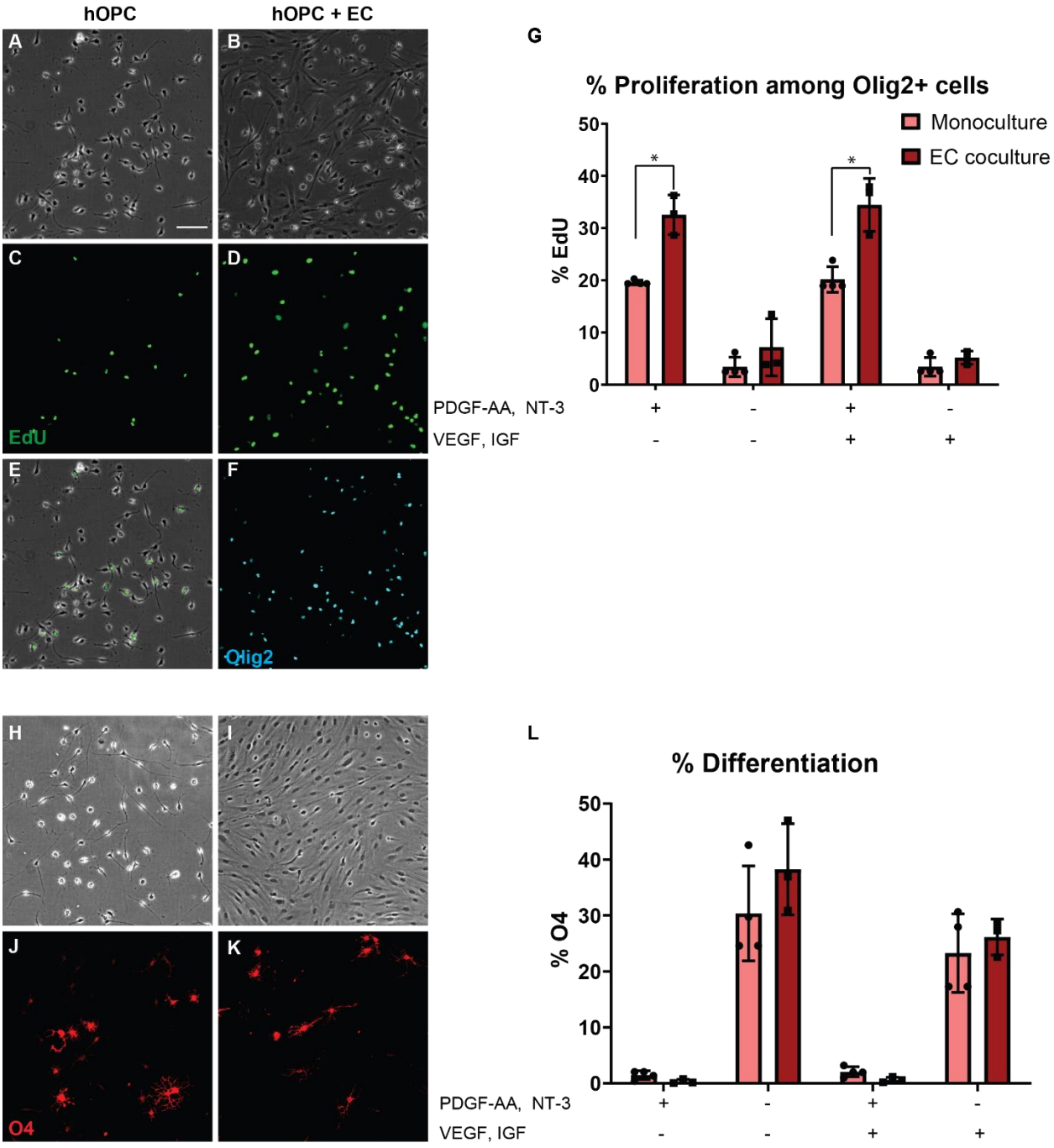

Figure 14: Effect of human endothelial cells on hOPC proliferation and differentiation. A, Mono-culture with only hOPCs B, Co-culture between hOPC and human Endothelial Cells C, Proliferation of hOPCs represented by EdU staining D, Proliferation of the co-culture condition represented by EdU staining E, Composite F, Olig2^{+} cells labelling hOPCs in co-culture condition condition G, human Endothelial Cells increases proliferation of hOPCs (2-way ANOVA, Mixed effects model, Holm-Sidak's multiple comparisons test, $p<0.0001$) H, Mono-culture with only hOPCs I, Co-culture between hOPCs and human Endothelial Cells J, O4+ differentiated oligodendrocytes in the hOPC mono-culture K, O4+ differentiated oligodendrocytes in co-culture L, human endothelial cells does not affect hOPC differentiation Scale 100µm

6 Discussion, Conclusion and Future Direction

Acetylcholine is a well-known neurotransmitter that is required for neuronal signal transduction. Apart from its release from cholinergic neurons, ACh from macrophages and dendritic cells is known to reduce inflammation by decreasing the amount of pro-inflammatory cytokines by autocrine action. This happens through the Cholinergic, Anti-inflammatory pathway (CAIP) [50, 51]. Glial ACh helps in providing nutritional support to neurons and also in maintenance of the BBB [52, 53]. Recent studies in our lab have primarily focused on understanding the function of muscarinic receptor signaling in Oligodendrocyte progenitor cells. We have shown previously that muscarinic agonists inhibit hOPC differentiation through its action on M3R receptor. We examined the regulation and effect of a precursor molecule to ACh; ChAT on hOPCs during remyelination. This would enable us to identify better therapeutic targets to enhance OPC differentiation.

We first investigated the cellular source of ACh during remyelination using lysolecithin induced focal demyelination model. Using a BAC transgenic ChAT GFP mouse, we identified increasing number of ChAT expressing cells over increasing days post lesion. It is possible that inflammation caused due to lysolecithin and LPS might have triggered neuronal and non-neuronal cells to release ACh to reduce the inflammatory activity around the lesion (CAIP). However, what effect this brings to the fate of hOPCs is a question of concern. Hence, it becomes absolutely necessary for us to understand active source of ACh after demyelination and the mechanisms that are associated with action of ACh on hOPC maturation during remyelination.

We identified injured and uninjured axons co-localizing with ChAT expression in focally demyelinated mice spinal cords suggesting neuronal sources of ACh as more predominant whereas we did not observe any clear co-localization among glial cell types, endothelial and pericytes. This remained consistent with different days post lesion and inflammation induced demyelination condition such as LPS intraspinal injection.

However, we cannot exclude the possibility of other sources of ACh such as immune cell types like T and B lymphocytes, which have been shown earlier to express ChAT [54, 55]. Thus identifying expression of ChAT amongst these lymphocytes during remyelination may give rise to further conclusive results.

Next, we investigated the basal ChAT expression levels in mouse brain across developmental stages. We observed ChAT expression levels to be 0.32% in P7, 0.21% in P14 and 1.3% in Adult mouse brain. However, future experiments aim to look at brain ChAT expression levels using Cuprizone based demyelination model. This will give better comparative results showing increasing ChAT expression with white matter injury in specific target organ.

Many recent research studies have shown that the cerebrovascular system is an intricate organization comprising of neurovascular niche [56], neuro-astro-vascular unit [57], oligo-vascular niche [21]; all of which contribute to major functions such as migration of progenitor cells, proliferation and differentiation into specific lineage. Specifically, Arai et al. demonstrated that endothelial cells under oxidative stress loses the ability to induce OPC proliferation. Studies have also shown that endothelial cells under exposure to fluid flow, releases ACh to promote flow mediated dilatation. This study suggested that, when

endothelial cells are under shear stress, they release ACh which acts as an autocrine signaling molecule to release vasodilatory substances like NO, Substance P etc.

Even though we have shown earlier that endothelial cells or pericytes do not express ChAT after lysolecithin demyelination or LPS inflammation inducing demyelination; we wanted to know if there may be other underlying factors that may trigger ACh release.

We thus, performed a flow cytometry analysis to observe ChAT expression among endothelial cells in different developing stages of mouse brain. The percentage of endothelial cells expressing ChAT was close to null in the uninjured state. However, CD31+GFP- cells that were sorted and seeded in vitro showed an upregulation in ChAT after 72 hours. This further indicates that there may be environment factors sthat could trigger the expression of ChAT in endothelial cells. Shear stress has also been shown to increase activity of NADPH oxidase 1 on endothelial cell membranes and thus increase superoxide production. This scheme has been observed in many MS patients who develop lesions [58].

We next wanted to identify if endothelial ACh affects hOPC proliferation and hOPC differentiation in a muscarinic dependent manner. To achieve this, we performed a co-culture between hOPCs and human endothelial cells. However, we did not see an effect on hOPC differentiation in comparison to a mono-culture of only hOPCs. This may be due to the presence of acetylcholine esterases that might have degraded ACh which was released from human endothelial cells. In order to test this, future experiments can be designed to add AChE inhibitor and observe hOPC differentiation. If we did see an effect on differentiation, we could further find out if this effect was dependent on muscarinic

signaling. To do this, we can treat co-cultures with darifenacin, a muscarinic antagonist and observe effect on hOPC differentiation.

It may be possible that human endothelial cells do not release ACh but mouse endothelial cells do (from the in vitro culture data). This then may be explained by a species specific difference in the release of ACh between mouse and human.

We observed an increase in the hOPC proliferation when they were co-cultured with human endothelial cells which indicates that factors released from endothelial cells promote hOPC proliferation. This was consistent with the data observed from the research by Arai et al. where they performed a co-culture between rat OPCs and human endothelial cells and observed a similar proliferation increase amongst the rat OPCs and showed evidence for involvement of Akt and Src signaling pathway.

Together, we conclude that, during remyelination, we observe an increase in the number of ChAT expressing cells and these cells are predominantly neuronal. This remain consistent with LPS inflammation induced demyelination. Through flow cytometry anaylsis, we detect a very small proportion of ChAT expression among mouse brain endothelial cells. However, sorting out GFP- endothelial cells and seeding in vitro, showed an upregulated ChAT expression after 72 hours. Better understanding of factors regulating endothelial ChAT expression may help us identify its possible action and effect on hOPCs. Further, presence of endothelial cells increases hOPC proliferation in a co-culture system. Perhaps targeting mechanisms that may strengthen this oligovascular niche may help in proliferation of hOPCs in the lesion site, providing therapeutic effect in demyelinating diseases like MS.

Appendix A: Reagents

1) Immunohistochemistry Recipes

10X PBS/T (PBS with thimerosal) (50 ml)

10X PBS	50	ml
thimerosal (Sigma T5125)	20	mg

Dilute 1:10 with *autoclaved* water for a 1X solution

Perm Buffer (50 ml)

10X PBS	5	ml
Tween-20 (0.25% Final)	125	µl
Triton X-100 (0.1% Final)	50	µl
Sterile water to 50 ml		ml

0.5% TritonX-100 BRAIN Blocking Buffer (50ml)

10X PBS/T	5	ml
Goat Serum (50%final)	25	ml
BSA (5% final)	2.5	ml
Triton X-100	250	µl
Sterile water to 50 ml		ml

0.5% TritonX-100 BRAIN SD (50ml)

10X PBS/T	5	ml
Goat Serum (25%final)	12.5	ml
BSA (2.5% final)	1.25	ml
Triton X-100	250	µl
Sterile water to 50 ml	31	ml

Sterile filter all solutions and store at 4 degrees.

2) Immunocytochemistry Recipes

10X PBS/T (PBS with thimerosal) (50 ml)

10X PBS	50	ml
thimerosal (Sigma T5125)	20	mg

Dilute 1:10 with *autoclaved* water for a 1X solution

0.01% TritonX-100 Blocking Buffer (50ml)

10X PBS/T	5	ml
Goat Serum (5%final)	2.5	ml
Triton X-100	5	□l
Sterile water to 50 ml		ml

0.01% TritonX-100 SD (50ml)

10X PBS/T	5	ml
Triton X-100	5	µl
Sterile water to 50 ml		

TritonX-100 0.1% Perm Buffer (50ml)

10X PBS/T	5	ml
Goat Serum (1% final)	500 ul	
Triton X-100	50	µl
Sterile water to 50 ml		

3) Tissue Dissociation Reagents

Pipes Working Solution

Make up solutions A & B:

[A] 10x stock of 1.2M NaCl, 50mM KCL Solution, **sterile filter, store at RT**

NaCl (MW 58.44, Biochem Stock Room)	10.52g	3.5g
KCL (MW 74.55, Biochem Stock Room)	0.559g	0.186g
ddH_20	to 150ml	to 50ml

[B] 0.5M Pipes buffer stock, **pH to 7.4**, **sterile filter, store at RT**

Pipes (Sigma P8658)	6.048g
1M NaOH	40mL

Mix together:

5ml	[A]
2ml	[B]
0.5ml	45% glucose (Sigma, G8769)
100 µl	0.5% sterile Phenol Red (Sigma, P0290-100mL)
To 50ml	sterile water

Sterile filter, store at RT wrapped in tin foil

Activated Papain

Papain (PAPL Worthington LS003126)	100 units
10x 11mM EDTA, 55mM L-cysteine-HCl (#2)	500 µL
Pipes Working Solution	4.5 ml

Mix, heat at 37◦C until clear, sterile filter

Sort Wash Buffer

PBS with 2mM EDTA and 0.5% BSA, **sterile filter, 4°C**

10 x PBS (VWR/Lonza, 12001-680), **pH7.2**	50
ddH_20	414
7.5% BSA (Invitrogen, 15260-037)	33.3
0.5M EDTA, pH 8 (VWR/MediaTech, 45001-122)	2
0.5% sterile Phenol Red (Sigma, P0290-100mL)	50
Total	500 ml

(Note: degassing is accomplished during sterile filtration)

10x stock of 11mM EDTA, 55mM l-cystein-HCl

0.5M EDTA, pH 8 (Invitrogen 15575-020)	220 µl
L-cystein-HCL (VWR/MP Biochemicals)	0.126 g
ddH_20	9.78 mL

4) Solochrome Cyanine Staining Solutions

Staining solution

0.21 M aqueous ferric chloride (5.6% w/v FeCl3.6H2O):	20 ml
Eriochrome cyanine R (Sigma):	1.0 g
Concentrated (95-98% w/w) sulfuric acid:	2.5 ml
Water:	to make 500ml

The ingredients take 2-5 minutes to dissolve, with stirring. Filter through whatman paper. The solution can be kept and used repeatedly for at least 8 years.

Differentiating solution

Ferric chloride (FeCl3.6H2O): 5.6% w/v
Add 5.6g ferric Chloride per 100 ml water.
The differentiating solution can be kept for a few years, but may be used only once.

Cell Culture Recipes

Poly-L-ornithine (Sigma-P3655-100MG)
Make 0.01% solution and store at 4C. (1 mg for every 10 ml sterile water). Use 500µL per well of 24 well plate. Incubate at 37ºC for three hours or overnight. Remove liquid and rinse twice with sterile dH_2O. Allow plates to dry in the hood. Store parafilm-wrapped plates at 4ºC or double coat.

Laminin (Invitrogen 23017-015 1 ml at 1 mg/ml)
Aliquot 50 µl per 1.5 ml vial on ice. Store aliquots at -20. To make a working stock, dilute 50 µl (50 ug) in 10 ml of cold HBSS(+) for a final concentration of 5µg/ml. To coat a poly-ornithine or poly-lysine 24 well plate, add 500µl per well. Incubate at 37ºC for three hours or overnight. Right before plating cells, aspirate laminin and wash once

with HBSS(+). Alternatively, after incubation wrap plate in parafilm store at 4°C for up to 1 week. Bring to room temperature before using and wash once with cold HBSS(+).

ND Media

Component	**Amount**	**Amount**	**Stock Conc.**	**Vendor**	**Catalog #**
DMEM/F12 L-Glutamine HEPES D-glucose Sodium Pyruvate Putrescine 2HCl NEAA	120 mL	240 mL	1x 2.5 mM 15 mM 17.51 mM 0.5 mM 81 µg/mL 0.05–0.25 mM	VWR/ MediaTech	45000-350
Neurobasal media	120 mL	240 mL		Invitrogen	21103-049
Sodium Pyruvate	2.5 mL	5 mL	100 mM	VWR/Lonza	12001-636
L-Glutamine	2.5 mL	5 mL	200 mM	VWR/Lonza	12001-698
Pen/strep	2.5 mL	5 mL	10,000 U/mL	VWR/Lonza	12001-692
N2 Insulin Transferrin Progesterone Putrescine Selenite	2.5 mL After filter	5 mL	100x 500 µg/mL 10,000 µg/mL 0.73 µg/mL 1600 µg/mL 0.5 µg/mL	Invitrogen	17502-048
Selenite	56.8 µL	113.6 µL	0.22 µg/µL	Sigma	S9133-1MG
Progesterone	7.5 µL	15 µL	2 µg/µL	Sigma	P6149-1MG

Trace Elements B	250 µL	500 µL	1000x	VWR/MediaTech	45000-714
Biotin	50 µL	100 µL	50 ng/µL	Sigma	B4639-500MG
B-27 Supplement	5.0 mL After filter	10 mL	50x	Invitrogen	17504-044
N-acetyl cysteine	250 µL	500 µL	5 mg/mL	Sigma	A8199-10G
	250 mL	**500 mL**			

Complete EGM Media (For Endothelial Cells)

PromoCell Catalog Number: C-22121

Fetal Calf Serum	0.05 ml/ml
Epidermal Growth Factor	5 ng/ml
Fibroblast Growth Factor	10 ng/ml
Insulin Like Growth Factor	20 ng/ml
Vascular Endothelial Growth Factor	0.5 ng/ml
Ascorbic Acid	1 µg/ml
Hydrocortisone	0.2 µg/ml

Add 0.2% Pennicilin and streptomycin (Biochemistry Stock Room). Add AbAM (VWR-12001-712) as a fungizone

Appendix B: Detailed Protocols

Mouse Brain dissociation

1. Administer Fatal+ (Sodium phenobarbital) through IP injection 100 µL of a 1:10 stock solution to sacrifice mouse. Do a cervical dislocation as a secondary method to confirm death. Using a scalpel blade, cut through the neck. Using scissors, incise the skin of the skull region. Remove any meninges that surrounds the skull. Using scissors, make a cut through the skull and remove the skull using forceps. Using spatula, scoop out the brain and store in HBSS(+)
2. Remove brain from the skull with a sterile spatula and carefully put it into a 50 ml tube filled with HBSS (+) with 0.4% Pen Strep.
3. Wash whole tissue (**recommend using only cortex to minimize myelin debris**) at least 3 times in cold in HBSS(+).
4. Remove most of HBSS+ as possible then pour tissue into sterile 100mm petri dish on a cold tray in the hood.
5. Remove any clots with sterile forceps.
6. Dissect brain into coronal 'bread' slices approximately 2 mm thick, place on side and use needle blades to remove corpus callosum and regions of white matter. Discard cerebellum. Transfer grey matter (cortices and subcortical tissue) using a pre-wetted sterile transfer pipet to fresh 100ml petri dish with minimal HBSS+ volume to facilitate step 7.
7. Mince tissue using #10 scalpel blades in a scissor motion.
8. Collect 1.5ml aliquots of tissue with a disposable sterile squeeze bulb pipette and add to 15 mL conical vial. Add a small volume of HBSS(+) to collect *all* tissue from dish.
9. Fill to 8 mL with HBSS(-). Cap the tube and invert 3 times to mix.
10. Let tubes sit and tissue sink. Spin 20 seconds at 2 clicks if pieces continue to float.
11. Remove the HBSS(-) down to the 2 mL mark and repeat Step 9 and 10.
12. Prepare **Activated Papain** and filter sterilize.
13. Remove the HBSS(-) supernatant down to the 2.5ml mark and add 2.5ml **Pipes Working Solution.** Cap the tube and invert 3 times to mix.
14. Quick spin 20 seconds at 2 clicks then remove supernatant completely.
15. Add **Pipes Working Solution** to the 2.5ml mark.
16. Add 2.5ml of **Activated Papain** (Total volume is now 5ml).
17. Invert the tube 3 times to mix and flick the tube to release stuck tissue from the conical part of the tube. Place the tubes horizontally in the 37°C incubator for 30 minutes to 1 hour. Roll tubes every 10 minutes. (begin making L,M,S pipettes)
18. At this time coat your tissue flasks with collagen (5ug/ml) and leave in 37 deg incubator for 20 minutes. Then wash the flasks with Milli-q water twice and leave it for air drying.

19. Remove the tubes from 37°C and add 2 ml of DMEM/F12 and 70uL **DNaseI.** Invert to mix and return tubes to incubator for 5 minutes. Additional DNaseI may be necessary.
20. Use a 5ml serological pipette to resuspend (slowly) and to mix (quickly) the tissue. Each tube should take less than 2 minutes to complete.
21. Spin 10 min at 260g (3 clicks). During the spin, make glass pipets (L, M, S). Keep sterile.
22. Aspirate the media down to 2 ml mark (now have 2ml of tissue & media).
23. Triturate the tissue with the pre-wet L, M, and S pipettes. Ten up and down with L, 5 with M and 2 with S. Trituration ~5 min or less per tube.
24. Prewet a 70um filter on a 50 ml conical vial with DMEM/F12 (~3ml media).
25. Dilute the tissue with DMEM/F12 up to 10ml PER 15 ML CONICAL before filtering.
26. FILTER **ONE** 15 ML CONICAL INTO **ONE** 50 ML CONICAL.
27. Wash filter with 3mL media before discarding.
28. Bring each tube to the maximum volume with DMEM/F12.
29. Spin at 260g for 10min (3 clicks).
30. Remove media to 5 ml mark and resuspend with 5ml pipet (Add 50 ul of DNaseI and place at 37 °C for 5 minutes if DNA clumps are present).
31. Bring the tube to the maximum volume with DMEM/F12.
32. Spin at 260g for 10min (3 clicks).
33. Resuspend in cold sort wash buffer (see Table below)

Myelin Removal (immediately following dissociation)

Keep cells cold (2-8 deg) and use pre-cooled solutions for all steps. This will prevent capping of antibodies on the cell surface and non-specific cell labeling.

Mouse	**<2 weeks old**	**2–3 weeks old**	**>3 weeks old**
Weight	300 mg	400 mg	500 mg
Sort Wash Buffer per whole mouse brain	180 µL	1080 µL	1800 µL
Myelin Removal Beads II per whole mouse brain	20 µL	120 µL	200 µL
LS Columns required	1 (for up to 2 brains)	2	3

1) Add volume of Myelin Removal Beads II as according to table above.
2) Mix well using 2ml pipette. Do not vortex. Incubate for 15 minutes in the cold room on the nutator.

3) Wash cells by adding 10× the labeling volume of buffer and centrifuge at 230-260g for 10 minutes (3 clicks). Aspirate supernatant completely.
4) Resuspend pellet in 1000 µL of buffer per each LS Column. [For example, if you need 3 LS Columns according to the table, add 3000 µL of buffer to the cell pellet (3×1000 µL) and apply 1000 µL to each LS Column.]
5) Pass cells through 70 µm nylon mesh to remove cell clumps which may clog the column. Moisten filter with Sort Wash buffer before use.
6) Place LS Column in the magnetic field of a suitable MACS Separator. For details refer to LS Column data sheet.
7) Prepare column by rinsing with 3 mL of buffer.
8) Apply cell suspension onto the column.
9) Collect unlabeled cells that pass through and wash column with 2×1 mL of buffer. Collect total effluent; this is the unlabeled cell fraction. Perform washing steps by adding buffer two times. Only add new buffer when the column reservoir is empty.
10) Count cells using a hemocytometer
11) Centrifuge the effluent at 230-260g for 7 mins (3 clicks) and resuspend based on experiment

References

1. Suzuki, K. and Y. Suzuki, *Globoid cell leucodystrophy (Krabbe's disease): deficiency of galactocerebroside β-galactosidase.* Proceedings of the National Academy of Sciences, 1970. **66**(2): p. 302-309.
2. Bjartmar, C., J. Wujek, and B. Trapp, *Axonal loss in the pathology of MS: consequences for understanding the progressive phase of the disease.* Journal of the neurological sciences, 2003. **206**(2): p. 165-171.
3. Sim, F.J., et al., *The age-related decrease in CNS remyelination efficiency is attributable to an impairment of both oligodendrocyte progenitor recruitment and differentiation.* Journal of Neuroscience, 2002. **22**(7): p. 2451-2459.
4. Franklin, R.J., *Why does remyelination fail in multiple sclerosis?* Nature Reviews Neuroscience, 2002. **3**(9): p. 705.
5. HALL, S.M., *The effect of injections of lysophosphatidyl choline into white matter of the adult mouse spinal cord.* Journal of cell science, 1972. **10**(2): p. 535-546.
6. Torkildsen, Ø., et al., *The cuprizone model for demyelination.* Acta Neurologica Scandinavica, 2008. **117**: p. 72-76.
7. Constantinescu, C.S., et al., *Experimental autoimmune encephalomyelitis (EAE) as a model for multiple sclerosis (MS).* British journal of pharmacology, 2011. **164**(4): p. 1079-1106.
8. Bothwell, M., *Mechanisms and medicines for remyelination.* Annual review of medicine, 2017. **68**: p. 431-443.
9. Gaesser, J.M. and S.L. Fyffe-Maricich, *Intracellular signaling pathway regulation of myelination and remyelination in the CNS.* Experimental neurology, 2016. **283**: p. 501-511.
10. Tawk, M., et al., *Wnt/β-catenin signaling is an essential and direct driver of myelin gene expression and myelinogenesis.* Journal of Neuroscience, 2011. **31**(10): p. 3729-3742.
11. Wahl, S.E., et al., *Mammalian target of rapamycin promotes oligodendrocyte differentiation, initiation and extent of CNS myelination.* Journal of Neuroscience, 2014. **34**(13): p. 4453-4465.
12. Zinnitz, F. and O. Hammer, *Cholinesterase, myelin and the treatment of multiple sclerosis.* Zeitschrift fur die gesamte innere Medizin und ihre Grenzgebiete, 1959. **14**: p. 901.
13. Kim, S., T. Oh, and D. Johnson, *Developmental changes of acetylcholinesterase and pseudocholinesterase in organotypic cultures of spinal cord.* Experimental neurology, 1972. **35**(2): p. 274-281.
14. Cree, B.A., et al., *Clemastine rescues myelination defects and promotes functional recovery in hypoxic brain injury.* Brain, 2017. **141**(1): p. 85-98.
15. Liu, J., et al., *Clemastine enhances myelination in the prefrontal cortex and rescues behavioral changes in socially isolated mice.* Journal of Neuroscience, 2016. **36**(3): p. 957-962.
16. Green, A.J., et al., *Clemastine fumarate as a remyelinating therapy for multiple sclerosis (ReBUILD): a randomised, controlled, double-blind, crossover trial.* The Lancet, 2017. **390**(10111): p. 2481-2489.
17. Lounkine, E., et al., *Large-scale prediction and testing of drug activity on side-effect targets.* Nature, 2012. **486**(7403): p. 361.
18. Abiraman, K., et al., *Anti-muscarinic adjunct therapy accelerates functional human oligodendrocyte repair.* Journal of Neuroscience, 2015. **35**(8): p. 3676-3688.
19. Seo, J.H., et al., *Oligodendrocyte precursor cells support blood-brain barrier integrity via TGF-β signaling.* PLoS One, 2014. **9**(7): p. e103174.

20. Kirk, J., et al., *Tight junctional abnormality in multiple sclerosis white matter affects all calibres of vessel and is associated with blood–brain barrier leakage and active demyelination.* The Journal of pathology, 2003. **201**(2): p. 319-327.
21. Arai, K. and E.H. Lo, *An oligovascular niche: cerebral endothelial cells promote the survival and proliferation of oligodendrocyte precursor cells.* Journal of Neuroscience, 2009. **29**(14): p. 4351-4355.
22. Iijima, K., et al., *Transplanted microvascular endothelial cells promote oligodendrocyte precursor cell survival in ischemic demyelinating lesions.* Journal of neurochemistry, 2015. **135**(3): p. 539-550.
23. Conway, G.D., et al., *Histone deacetylase activity is required for human oligodendrocyte progenitor differentiation.* Glia, 2012. **60**(12): p. 1944-1953.
24. Pol, S.U., et al., *Sox10-MCS5 enhancer dynamically tracks human oligodendrocyte progenitor fate.* Experimental neurology, 2013. **247**: p. 694-702.
25. Proskocil, B.J., et al., *Acetylcholine is an autocrine or paracrine hormone synthesized and secreted by airway bronchial epithelial cells.* Endocrinology, 2004. **145**(5): p. 2498-2506.
26. Fujii, T., et al., *Expression and function of the cholinergic system in immune cells.* Frontiers in immunology, 2017. **8**: p. 1085.
27. Kirkpatrick, C.J., et al., *Expression and function of the non-neuronal cholinergic system in endothelial cells.* Life sciences, 2003. **72**(18-19): p. 2111-2116.
28. Grando, S.A., M.R. Pittelkow, and K.U. Schallreuter, *Adrenergic and cholinergic control in the biology of epidermis: physiological and clinical significance.* Journal of Investigative Dermatology, 2006. **126**(9): p. 1948-1965.
29. Kurzen, H., et al., *The non-neuronal cholinergic system of human skin.* Hormone and metabolic research, 2007. **39**(02): p. 125-135.
30. Tallini, Y.N., et al., *BAC transgenic mice express enhanced green fluorescent protein in central and peripheral cholinergic neurons.* Physiological genomics, 2006. **27**(3): p. 391-397.
31. McKay, J., W. Blakemore, and R. Franklin, *Trapidil-mediated inhibition of CNS remyelination results from reduced numbers and impaired differentiation of oligodendrocytes.* Neuropathology and applied neurobiology, 1998. **24**(6): p. 498-506.
32. Takeshita, Y. and R.M. Ransohoff, *Inflammatory cell trafficking across the blood–brain barrier: chemokine regulation and in vitro models.* Immunological reviews, 2012. **248**(1): p. 228-239.
33. Goverman, J., *Autoimmune T cell responses in the central nervous system.* Nature Reviews Immunology, 2009. **9**(6): p. 393.
34. Weiss, H.A., J.M. Millward, and T. Owens, *CD8+ T cells in inflammatory demyelinating disease.* Journal of neuroimmunology, 2007. **191**(1-2): p. 79-85.
35. Felts, P.A., et al., *Inflammation and primary demyelination induced by the intraspinal injection of lipopolysaccharide.* Brain, 2005. **128**(7): p. 1649-1666.
36. Desai, R.A., et al., *Cause and prevention of demyelination in a model multiple sclerosis lesion.* Annals of neurology, 2016. **79**(4): p. 591-604.
37. Friedman, W., et al., *Differential actions of neurotrophins in the locus coeruleus and basal forebrain.* Experimental neurology, 1993. **119**(1): p. 72-78.
38. Kamegai, M., et al., *Interleukin 3 as a trophic factor for central cholinergic neurons in vitro and in vivo.* Neuron, 1990. **4**(3): p. 429-436.
39. Gould, E. and L.L. Butcher, *Developing cholinergic basal forebrain neurons are sensitive to thyroid hormone.* Journal of Neuroscience, 1989. **9**(9): p. 3347-3358.
40. Contestabile, A., et al., *Choline acetyltransferase activity at different ages in brain of Ts65Dn mice, an animal model for Down's syndrome and related neurodegenerative diseases.* Journal of neurochemistry, 2006. **97**(2): p. 515-526.

41. Haberberger, R.V., M. Bodenbenner, and W. Kummer, *Expression of the cholinergic gene locus in pulmonary arterial endothelial cells.* Histochemistry and cell biology, 2000. **113**(5): p. 379-387.
42. López-Canales, J., et al., *Mechanisms involved in the vasorelaxant effects produced by the acute application of amfepramone in vitro to rat aortic rings.* Brazilian Journal of Medical and Biological Research, 2015. **48**(6): p. 537-544.
43. Wilson, C., M.D. Lee, and J.G. McCarron, *Acetylcholine released by endothelial cells facilitates flow-mediated dilatation.* The Journal of physiology, 2016. **594**(24): p. 7267-7307.
44. Shen, Q., et al., *Endothelial cells stimulate self-renewal and expand neurogenesis of neural stem cells.* Science, 2004. **304**(5675): p. 1338-1340.
45. Nakagomi, N., et al., *Endothelial cells support survival, proliferation, and neuronal differentiation of transplanted adult ischemia-induced neural stem/progenitor cells after cerebral infarction.* Stem cells, 2009. **27**(9): p. 2185-2195.
46. Tsai, H.-H., et al., *Oligodendrocyte precursors migrate along vasculature in the developing nervous system.* Science, 2016. **351**(6271): p. 379-384.
47. Niu, J., et al., *Aberrant oligodendroglial–vascular interactions disrupt the blood–brain barrier, triggering CNS inflammation.* Nature neuroscience, 2019. **22**(5): p. 709.
48. Hayakawa, K., et al., *Cerebral endothelial derived vascular endothelial growth factor promotes the migration but not the proliferation of oligodendrocyte precursor cells in vitro.* Neuroscience letters, 2012. **513**(1): p. 42-46.
49. Cohen, R.I., et al., *Nerve growth factor and neurotrophin-3 differentially regulate the proliferation and survival of developing rat brain oligodendrocytes.* Journal of Neuroscience, 1996. **16**(20): p. 6433-6442.
50. Parada, E., et al., *The microglial α7-acetylcholine nicotinic receptor is a key element in promoting neuroprotection by inducing heme oxygenase-1 via nuclear factor erythroid-2-related factor 2.* Antioxidants & redox signaling, 2013. **19**(11): p. 1135-1148.
51. Revathikumar, P., et al., *Immunomodulatory effects of nicotine on interleukin 1β activated human astrocytes and the role of cyclooxygenase 2 in the underlying mechanism.* Journal of neuroinflammation, 2016. **13**(1): p. 256.
52. Winkler, J., et al., *Essential role of neocortical acetylcholine in spatial memory.* Nature, 1995. **375**(6531): p. 484.
53. Parnavelas, J., W. Kelly, and G. Burnstock, *Ultrastructural localization of choline acetyltransferase in vascular endothelial cells in rat brain.* Nature, 1985. **316**(6030): p. 724.
54. Olofsson, P.S., et al., *Blood pressure regulation by CD4+ lymphocytes expressing choline acetyltransferase.* Nature biotechnology, 2016. **34**(10): p. 1066.
55. Rosas-Ballina, M., et al., *Acetylcholine-synthesizing T cells relay neural signals in a vagus nerve circuit.* Science, 2011. **334**(6052): p. 98-101.
56. Ohab, J.J., et al., *A neurovascular niche for neurogenesis after stroke.* Journal of Neuroscience, 2006. **26**(50): p. 13007-13016.
57. Meshulam, L., et al., *The role of the neuro-astro-vascular unit in the etiology of ataxia telangiectasia.* Frontiers in pharmacology, 2012. **3**: p. 157.
58. Fischer, M.T., et al., *NADPH oxidase expression in active multiple sclerosis lesions in relation to oxidative tissue damage and mitochondrial injury.* Brain, 2012. **135**(3): p. 886-899.